

2011
2012

GENEESKUNDE

*master in de biomedische wetenschappen: klinische
moleculaire wetenschappen*

Masterproef

Cell therapy in neonatal hypoxic ischemic encephalopathy

Promotor :
prof. dr. BORIS W. KRAMER

Stephanie De Munter

*Masterproef voorgedragen tot het bekomen van de graad van master in de biomedische
wetenschappen , afstudeerrichting klinische moleculaire wetenschappen*

De transnationale Universiteit Limburg is een uniek samenwerkingsverband van twee universiteiten in twee landen:
de Universiteit Hasselt en Maastricht University

universiteit
hasselt
KNOWLEDGE IN ACTION

 Maastricht University

Universiteit Hasselt | Campus Diepenbeek | Agoralaan Gebouw D | BE-3590 Diepenbeek
Universiteit Hasselt | Campus Hasselt | Martelarenlaan 42 | BE-3500 Hasselt

 Maastricht University

universiteit
hasselt
KNOWLEDGE IN ACTION

2011
2012

GENEESKUNDE

*master in de biomedische wetenschappen: klinische
moleculaire wetenschappen*

Masterproef

Cell therapy in neonatal hypoxic ischemic encephalopathy

Promotor :
prof. dr. BORIS W. KRAMER

Stephanie De Munter

*Masterproef voorgedragen tot het bekomen van de graad van master in de biomedische
wetenschappen, afstudeerrichting klinische moleculaire wetenschappen*

Table of contents

Abbreviations	3
Abstract.....	5
1. Introduction	7
1.1 Perinatal hypoxic-ischemic brain injury	7
1.2 Pathophysiology of hypoxic-ischemic brain injury	7
1.2.1 Excitotoxicity and free radical attack	7
1.2.2 The systemic response.....	8
1.2.3 Cellular components of hypoxic-ischemic brain injury.....	8
1.3 Neuroprotective strategies.....	9
1.3.1 Treatment options.....	9
1.3.2 Stem cell therapy	9
1.4 This thesis.....	11
1.4.1 Animal model	11
1.4.2 Preliminary data.....	11
1.4.3 Hypothesis and research question	11
1.4.4 Experimental approach.....	12
2. Materials and methods	13
2.1. Experimental groups.....	13
2.2 Experimental design	13
2.3 Stem cell and G-CSF preparations.....	15
2.4 Histology tissue preparation	15
2.5 Area estimates.....	16
2.6 Nissl staining.....	16
2.7 Immunohistochemistry.....	16
2.8 Neuropathological examination	17
2.8.1 Quantitative analysis of synaptophysin staining.....	17
2.8.2 Calculation of the presynaptic bouton density.....	17
2.8.3 Quantitative analysis of IBA-1 staining.....	18
2.8.4 Quantitative analysis of O4 staining	18
2.9 Statistical analysis	18

3. Results.....	19
3.1 Baseline characteristics.....	19
3.2 Objective 1: hypoxic-ischemic damage to the preterm brain	20
3.2.1 Brain weight	20
3.2.2 Hippocampal atrophy.....	20
3.2.3 Presynaptic bouton density	21
3.2.4 Neurons	23
3.2.5 Microglial density in the hippocampus.....	24
3.2.6 Microglial density in the periventricular white matter	26
3.2.7 White matter O4 expression	27
3.3 Objective 2: MSC and G-CSF therapies in neonatal hypoxic-ischemic encephalopathy	28
3.3.1 Brain weight.....	28
3.3.2 Hippocampal atrophy.....	29
3.3.3 Presynaptic bouton density	30
3.3.4 Neurons	32
3.3.5 Microglial density in the hippocampus.....	33
3.3.6 Microglial density in the periventricular white matter	35
3.3.7 White matter O4 expression	37
4. Discussion	39
5. Conclusion and synthesis.....	45
References	47
Acknowledgements	51
Supplement	53
Supplement A	53
Supplement B	55

Abbreviations

AMPA	α -Amino-3-hydroxy-5-Methylisoxazole-4-Propionic Acid
ATP	Adenosine-5'-Triphosphate
CA	Cornu Ammonis
CNS	Central Nervous system
DAB	Diaminobenzidine
DG	Dentate gyrus
DMSO	Dimethyl Sulfoxide
EEG	Electro-encephalogram
ECG	Electrocardiogram
FCS	Fetal Calf serum
GA	Gestational age
G-CSF	Granulocyte-Colony Stimulating Factor
H₂O₂	Hydrogen peroxide
HC	Hippocampus
HI	Hypoxic Ischemia/ Hypoxic-Ischemic
HIE	Hypoxic-Ischemic Encephalopathy
HSC	Hematopoietic Stem Cells
hu-BM-MSC	human Bone Marrow derived Mesenchymal Stem Cells
IBA-1	Ionized calcium Binding Adaptor molecule 1
I.V.	Intravenous
MSC	Mesenchymal Stem Cells
NMDA	N-Methyl-D-Aspartate
PVWM	Periventricular White Matter
RNS	Reactive Nitrogen Species
ROS	Reactive Oxygen Species
SAL	Saline
SD	Standard deviation
SG	Stratum Granulosum
SL	Stratum Lucidum
SM	Stratum Moleculare
SR	Stratum Radiatum
TBS	Tris Buffered Saline
TBS-T	Tris Buffered Saline Triton
UCO	Umbilical Cord Occlusion
VSI	Virtual Slide Image
WHO	World Health Organization

Abstract

Introduction: Perinatal hypoxic-ischemic encephalopathy (HIE) is a major cause of preterm brain injury. In the Western world, there has been a tremendous increase in preterm birth rates over the past 20 years and the incidence of perinatal HIE is estimated at two to six per 1000 live-born infants. Currently, few treatment options are available for preterms suffering from HIE. In this translational research project, we hypothesize that Mesenchymal Stem Cells (MSC) and Granulocyte-Colony Stimulating Factor (G-CSF) therapies can reduce hypoxic-ischemic related synapse loss, neurodegeneration, microglial proliferation and damage to pre-oligodendrocytes in a fetal sheep model, thereby limiting preterm HIE.

Materials and methods: Time-mated ewes with singleton fetuses at a gestational age of 102 days (term = 145 days) were randomly assigned to receive either global hypoxic-ischemia (HI) through 25 minutes of umbilical cord occlusion or no HI. Occlusion was followed by a reperfusion period of seven days. Within each group, fetuses received MSC, G-CSF or a sham treatment (saline). Cerebral weight and hippocampal area were determined. Brain injury was quantified by immunohistochemical staining of synapses, neurons, microglia and pre-oligodendrocytes. Cellular damage patterns were evaluated in the fetal hippocampus and the periventricular white matter (PVWM).

Results: Cerebral weight and hippocampal area were significantly reduced following global HI. In occluded animals, presynaptic bouton densities were significantly increased in all hippocampal regions. MSC or G-CSF therapy showed no additional effects. Morphological analysis showed a well-defined layer of neuronal cell bodies surrounded by a strong synaptic staining pattern in all hippocampal regions of control animals. Following HI, the normal distribution of neurons and synapses was markedly disturbed. MSC transplantation was associated with a clear trend towards ultrastructural repair. Results were less outspoken following G-CSF treatment. Quantitative analysis of microglial density in the fetal hippocampus and PVWM revealed a significant increase after global HI. Decreasing trends were observed following MSC or G-CSF therapy. Pre-oligodendrocyte number was significantly decreased in the PVWM of occluded animals, while cells in the MSC-occlusion group were preserved.

Conclusions: The present study demonstrates that a global HI insult for 25 minutes, followed by a seven day reperfusion period, is associated with changes in synaptic circuitries, neuronal damage and profound microglial proliferation and activation in the developing hippocampus. In addition, we present that white matter injury is associated with microglial proliferation and loss of non-myelinating pre-oligodendrocytes. Together, these data illustrate the massive impact of systemic HI on the preterm brain. MSC transplantation and G-CSF administration showed moderate hippocampal repair. The therapeutic effect of MSC therapy was visible in the PVWM, as pre-oligodendrocytes were spared following HI.

Abstract

Introductie: Perinatale hypoxische ischemische encefalopathie (HIE) is een veel voorkomende oorzaak van premature hersenschade. In de Westerse wereld is het aantal premature geboortes de laatste 20 jaar enorm toegenomen en de incidentie van perinatale HIE wordt geschat op twee tot zes per 1000 kinderen. Momenteel zijn er slechts weinig behandelingsopties voor prematuren met HIE. In dit translationeel onderzoeksproject werd de volgende hypothese voorop gesteld: 'Toediening van Mesenchymale Stamcellen (MSC) of Granulocyt-Kolonie stimulerende Factor (G-CSF) kan het verlies van synapsen, neurodegeneratie, microglia proliferatie en schade aan pre-oligodendrocyten, veroorzaakt door globale hypoxische ischemie (HI), voorkomen in een foetaal schapenmodel. Bijgevolg verwachten we dat beide therapieën in staat zijn tot het limiteren van premature HIE.

Materiaal en methoden: Bij een zwangerschapsduur van 102 dagen (voltijdse dracht = 145 dagen) werden foetale lammeren al dan niet onderworpen aan globale HI, hetgeen geïnduceerd werd door middel van occlusie van de navelstreng (25 minuten). Occlusie werd opgevolgd door een reperfusie periode van zeven dagen. In elke groep ontvingen de foetussen een van de volgende behandelingen: MSC, G-CSF of een zoutoplossing. Hersengewicht en hippocampusoppervlak werden bepaald. Cerebrale schade werd geëvalueerd in de foetale hippocampus en periventriculaire witte stof (PVWM).

Resultaten: Hersengewicht en hippocampusoppervlak waren beiden significant gedaald na globale HI. In geoccludeerde dieren was de densiteit van presynaptische vesikels significant gestegen in alle hippocampale regio's. MSC of G-CSF therapie toonde geen additionele effecten. Morfologische analyses in alle hippocampale regio's van controle dieren toonde een duidelijk gedefinieerde neuronale laag aan die rijkelijk omgeven werd door synapsen. Na HI was de normale distributie van neuronen en synapsen grondig verstoord. MSC transplantatie ging samen met een duidelijk herstel van de gelaagdheid in deze gebieden. Resultaten waren minder uitgesproken na de G-CSF behandeling. Kwantitatieve analyse van de microgliale densiteit in de foetale hippocampus en PVWM onthulde een significante stijging na occlusie. Dalende trends werden waargenomen na MSC of G-CSF therapie. Systemische HI ging gepaard met een significante daling in het aantal pre-oligodendrocyten in de PVWM, terwijl het aantal cellen bewaard bleef in de MSC-occlusie groep.

Conclusie: Deze studie toont aan dat globale HI, gevolgd door een zevendaagse reperfusie periode, gepaard gaat veranderingen in synaptische circuits, neuronale schade en duidelijke microglia proliferatie en activatie in de immature hippocampus. Daarnaast stellen we vast dat witte stof schade geassocieerd kan worden met microglia proliferatie en het verlies van pre-oligodendrocyten. Deze data tonen de massieve impact van globale HI op een premature brein aan. MSC transplantatie en G-CSF administratie hadden beiden geringe effecten op het herstel in de hippocampus. MSC therapie toonde een therapeutisch effect in de PVWM.

1. Introduction

1.1 Perinatal hypoxic-ischemic brain injury

Preterm babies are at high risk of neurodevelopmental complications during the perinatal period (1). Perinatal asphyxia, initiated by a lowered perfusion pressure and followed by reperfusion, is correlated to pronounced brain injury and poor outcome (2). According to the World Health Organization (WHO), approximately 900.000 deaths are related to birth asphyxia each year making it a major contributor to early neonatal mortality (3). In the Western world, there has been a tremendous increase in preterm birth rates over the past 20 years (4) and the incidence of perinatal Hypoxic-Ischemia (HI) is estimated at two to six per 1000 live-born infants (2, 5, 6). In developing countries, however, these numbers are much higher (7, 8).

Impaired blood gas exchange is closely linked to three biochemical components namely hypoxemia, hypercapnia and metabolic acidosis (9). The main pathogenic mechanisms contributing to fetal blood flow interruption include maternal problems (e.g. hypotension, uterine trauma or diabetes) as well as nuisances related to the placenta (e.g. abruption placentae) or the umbilical cord (e.g. umbilical cord compression). Beside these, it is possible that the causality is infant-related (e.g. a compromised fetus that does not tolerate the stress of labor or failure to expand the lungs right after birth) (10). In general, fetal distress prior to delivery, resuscitation at birth, abnormal Apgar scores, multi-organ systemic disease and several well-defined neurologic signs (e.g. feeding difficulties and seizures) are utilized as criteria to determine if the neonate suffered from HI-related brain damage (9). Depending on the severity of the symptoms, Hypoxic-Ischemic Encephalopathy (HIE) can be mild, moderate or severe. Mild HI brain injury is usually not associated with long-term neurological deficits. Early childhood, however, may be characterized by impairments in motor development and an altered level of consciousness. Infants with moderate HIE have a 30% risk on developing (motor) disabilities, while intellectual properties are commonly preserved. In general, children do not survive severe HI-related brain damage. Among survivors, many, if not all, have mental as well as motor handicaps. On average, 15 - 20% of all infants with HIE die in the neonatal period and another 25% develop significant neurologic sequelae (11).

1.2 Pathophysiology of hypoxic-ischemic brain injury

Although the pathophysiological impact of HI still remains to be clarified, evidence shows that a detrimental combination cerebral inflammation and the host immune response determine the extent of brain injury following global HI. HI induces a series of molecular, systemic and cellular responses that either result in adaptation and survival or cell death.

1.2.1 Excitotoxicity and free radical attack

Oxygen and glucose deficiencies following blood flow perturbations result in cerebral energy failure and a cascade of biochemical events. When mitochondrial dysfunction persists, several neurotransmitters are released. During HI, perturbations in neuronal depolarization result in high levels of glutamic acid which is cytotoxic to neuronal cells and is involved as etiological agents in neuronal

injury. The simultaneous decrease in glutamate-dependent adenosine-5'-triphosphate (ATP)ase in presynaptic membranes keeps the extracellular glutamate levels high. Together, these events cause a protracted excitement of the glutamate receptors. The N-Methyl-D-Aspartate (NMDA) and the α -Amino-3-hydroxy-5-Methylisoxazole-4-Propionic Acid (AMPA) receptors are major contributors in regulating the activity of excitatory amino acids. Concurrent activation of the NMDA and the glycine receptors results in elevated cytosolic calcium levels. As calcium activates degrading enzymes (e.g. endonucleases, proteases and phospholipases), the abovementioned process is the major trigger in HI and reperfusion induced cell death. Beside this, increased intracellular calcium concentrations may trigger free radical generation which in turn causes the release of additional amounts of neurotransmitters (10, 12-14). Although reperfusion is required to restrict cerebral damage, re-oxygenation triggers a cascade of compensatory biochemical events accompanied by oxidative stress (15, 16). The high levels of oxygen consumption, low levels of antioxidants and high concentrations of lipids predispose the preterm to oxidative damage (17).

1.2.2 The systemic response

Regardless of the cause of the HI insult, cardiac and vascular adjustments will ensue following prolonged hypoxia. Redistribution of the cardiac output results in hypotension, ischemia and an anaerobic metabolism. Therefore, hypoxia is a cause as well as a consequence of ischemia. Systemic changes (e.g. a reduced perfusion of peripheral tissues and abdominal viscera) occur in order to protect perfusion of the heart and the Central Nervous System (CNS). Nonetheless, severe HI also significantly affects these organs resulting in clinical manifestations. The underdeveloped cerebrovascular system and the high energy demands of the developing brain make it particularly sensitive for oxygen and nutrient deprivation (18).

1.2.3 Cellular components of hypoxic-ischemic brain injury

Alterations ensuing an ischemic event can also be ascertained at a cellular level. In the CNS, resident microglia are the first non-neural cells that rapidly respond to pathology. Following cerebral ischemia, these glial cells exert a cytotoxic function by releasing Reactive Oxygen Species (ROS), Reactive Nitrogen Species (RNS) and inflammatory cytokines, thereby inducing neuronal damage. Previous investigations suggested a correlation between microglial activation and the severity of ischemic injury. On the other hand, these phagocytic and immunocompetent cells may be involved in neuroprotection by producing neurotrophic factors and by eliminating deleterious cellular debris (19, 20). In addition, the systemic inflammatory response is a well-known phenomenon induced by various toxic insults to the body. Blood-derived leukocytes and macrophages are considered the main inflammatory cells accumulating within the brain 12 to 24 hours after ischemia (20). Numerous animal models of stroke declare that, among leukocytes, neutrophils are the major mediators involved in the second phase of HI-related brain injury. In addition, other peripheral inflammatory cells like mononuclear phagocytes, T-lymphocytes and natural killer cells also contribute to CNS inflammation and gliosis by producing and secreting damaging cytokines (21, 22).

The neuropathological features of neonatal HIE are determined by several factors such as the metabolic status, including temperature, and the duration of the HI insult (23). A major form of brain damage associated with prematurity is periventricular white matter (PVWM) injury involving diffuse astrogliosis with subsequent loss of pre- and immature oligodendrocytes (24, 25). Additional laboratory data show a decrease in both pre- and postsynaptic densities in the neonatal brain immediately after the ischemic insult (26, 27). Moreover, detrimental effects on immature neurons and endothelial cells have been described (21, 28). The neuropathology includes deep grey matter injury, particularly to the neurocircuitries of the hippocampus and the basal ganglia, with relative sparing of the cortex (29, 30).

1.3 Neuroprotective strategies

1.3.1 Treatment options

Nowadays, perinatal care of asphyxiated neonates is restricted to the retention of oxygen equilibrium, monitoring of blood pressure, controlling seizures and managing of intracranial hypertension (31). When intervention starts early, hypothermia has moderate neuroprotective effects on term infants with mild HI brain damage (32-34). However, treatment options for preterm babies are still limited (35-38). This emphasizes the importance of new therapeutic strategies with the ability to reduce brain injury in asphyxiated preterms.

The HI-related inflammatory response has bipartite characteristics as it exacerbates cerebral damage while it is also indispensable in removing cell debris and in initiating regenerative processes. Typically, these reactions have a rapid onset and continue after cerebral ischemia. Intervening with the causative compounds might have profound implications for patient treatment as this can diminish the progression of brain injury during the late stages of cerebral ischemia (21). Currently, cell therapies are an up-to-date and promising approach to treat neurological diseases.

1.3.2 Stem cell therapy

Administration of exogenous stem cells

Stem cells are characterized by their ability to self-renew and to differentiate into various specialized cell types. Adult multipotent progenitor cells reside within specialized regions of the postnatal brain namely the dentate gyrus (DG) of the hippocampus and the subventricular zone (SVZ) of the lateral ventricles. Upon brain injury, neurogenic brain regions show profound cell proliferation and neurogenesis is stimulated in both the DG and the SVZ. However, these endogenous repair mechanisms are not sufficient to re-establish cerebral cell loss following HI (39, 40).

Bone marrow contains, at least, two cell populations with great potential for clinical use: Mesenchymal Stem Cells (MSC) and Hematopoietic Stem Cells (HSCs) (35). MSCs are spindle-shaped, multipotent cells with a fibroblast-like morphology that are ubiquitously present. In addition to bone marrow and adipose tissue, which are the major adult cell sources, amniotic fluid and the Wharton jelly of the umbilical cord also appear to be rich sources of MSCs. These cells have the ability to differentiate into cells of one germ layer, the mesoderm (41). Still, *in vitro* experiments have shown that they also have

the capacity to differentiate into cells that act as functional neurons, astrocytes or endothelial cells, a process known as transdifferentiation (42, 43).

The clinical application of MSCs is based on their property to modulate immune responses. MSCs regulate the immune system by influencing both the innate and the adaptive immunity wherein they target immune cells nonspecifically. By releasing anti-inflammatory cytokines, anti-apoptotic and trophic molecules, MSCs modify the microenvironment of damaged tissues. In addition, MSCs can also exert immune enhancing properties (41). Experimental studies involving MSC transplantation in neonatal mice that underwent cerebral HI showed promising results as MSC therapy improved functional recovery, reduced the cerebral lesion volume and decreased the number of proliferating inflammatory cells. In addition, MSCs can stimulate neurogenesis, the formation of new oligodendrocytes and synaptogenesis. However, the importance of engraftment and the necessity of transdifferentiation remain controversial (2, 35). Data about the clinical use of MSCs suggest that these cells are safe in terms of tumor formation and immune rejection (41). Because of the regenerative and anti-inflammatory capacities of MSCs, they may offer a novel therapeutic strategy for preterm brain damage following HI.

Mobilization of endogenous stem cells

The finding that multipotent HSCs, defined by their ability to give rise to all blood cell types, are capable to transdifferentiate into neuronal lineage has enlarged their scope of use (35). Granulocyte Colony-Stimulating Factor (G-CSF) is an endogenous peptide hormone of the hematopoietic system. By acting on bone marrow-derived stem cells, this growth factor has a major role in regulating the proliferation and differentiation of cells committed to the neutrophilic granulocyte lineage (44, 45). Yata *et al.*, reported that cerebral insults caused by HI in neonatal rats are accompanied by an increased neuronal expression of the G-CSF receptor (31). Recruiting stem cells to injured brain areas could be an indirect action mechanism involved in neural repair. Additionally, G-CSF-mediated brain protection might be attributed to its ability to stimulate intrinsic neural stem cells (46, 47). Several *in vivo* models of brain injury concluded that G-CSF seems to be involved in neurogenesis, neuroprotection and neural repair via neurotrophic, excitoprotective, anti-inflammatory and anti-apoptotic mechanisms (48-51). Therapeutic effects that have been attributed to G-CSF treatment in rodent models of ischemic stroke are: reduced cerebral edema, improved survival and an enhanced sensorimotor and functional recovery (47, 49, 52, 53). Currently, human malignancies of hematological origin are routinely treated with G-CSF (54), phase two dose-escalation clinical trials are assessed in patients with stroke (45) and experimental approaches are being tested in Multiple Sclerosis (55). Furthermore, no toxicity of G-CSF therapy in neonates with established systemic infection has been described (56). Regarding the aforementioned multimodal behavior of G-CSF and the fact that human treatments appear to be safe and well tolerated, this growth factor may have great potential for being a future treatment modality in HI-related injury to the preterm brain.

1.4 This thesis

In the present study, new neuroprotective strategies that are applicable in preterms suffering from HIE are investigated. For the purpose of this thesis, we will focus on MSC and G-CSF therapies. It is suggested that the tolerant immune system together with the growth directed environment and the permeable blood-brain barrier make preterm infants excellent candidates for cell based interventions.

1.4.1 Animal model

In order to study the outcome of HIE and to understand the results of MSC and G-CSF therapies on HI-induced brain injury, a unique animal model is used: systemic HI by umbilical cord occlusion (UCO) in preterm sheep fetuses. This model is commonly used in perinatology because the neurodevelopment of preterm sheep is comparable to that of preterm humans and this in terms of neurogenesis and the pattern of cerebral white matter myelination. In the current project, fetal sheep (0.7 GA) with a developmental stage comparable to a human pregnancy of 30 to 32 weeks was utilized. Additionally, the anatomic similarities and the quantity of cerebral white matter makes the fetal sheep an ideal model for studying human neuropathologic conditions (57). The size of the sheep fetus together with the long gestation period make it possible to apply chronic instrumentation (e.g. repeated access to blood and recording of fetal EEG) and to select a developmental stage that matches to the experimental demands (e.g. timing for the insult to be given and evaluated).

1.4.2. Preliminary data

Preliminary data of our lab show that human Bone Marrow-derived Mesenchymal Stem Cells (hu-BM-MSCs) and human recombinant G-CSF treatments preserve brain function, as measured by electroencephalography (EEG), in preterm sheep exposed to global HI (Jellema *et al.*, article in preparation). In addition, data confirmed that human recombinant G-CSF effectively mobilizes sheep white blood cells and HSCs.

1.4.3 Hypothesis and research question

Our research question is: "Are exogenous administered human Bone Marrow-derived Mesenchymal Stem Cells (hu-BM-MSCs) and human recombinant G-CSF therapies effective in reducing brain damage, caused by a global HI insult, in a preterm sheep model?" We subsequently hypothesize that both treatments can attenuate brain injury in HI sheep fetuses, in part by reducing synapse loss, neurodegeneration, pre-oligodendrocyte loss and by diminishing the activation and proliferation of resident microglia.

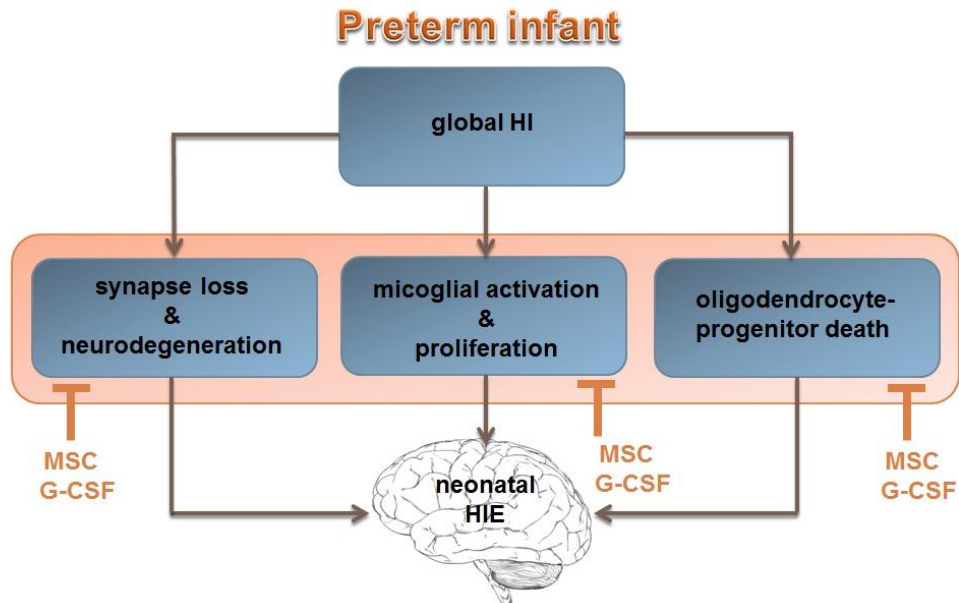


Figure 1: Hypothesis. We hypothesize that both MSC and G-CSF treatments can attenuate brain injury in hypoxic-ischemic sheep fetuses, in part by reducing neurodegeneration, synapse loss and pre-oligodendrocyte loss and by diminishing the activation and proliferation of resident microglia.

1.4.4 Experimental approach

In the first part of this thesis, HI cellular damage in the brain of preterm sheep was explored. Furthermore, the effectiveness of hu-BM-MSCs and human recombinant G-CSF therapies in reducing HI-related damage to the fetal sheep brain was investigated. Histological stainings for synapses, neurons, microglia and pre-oligodendrocytes were performed and analysis was conducted in the fetal hippocampus and PVWM. Results of this translational study will have implications in the development of a novel therapy for perinatal HIE in preterm infants.

2. Materials and methods

2.1. Experimental groups

Fetuses of time-mated Texel ewes ($n = 30$), gestational age (GA) of 102 ± 0.9 (mean \pm SD) days (term = 145 days), were randomly assigned to UCO (HI; $n = 18$) according to a procedure previously described by Roelfsema *et al.* (2004) (32) or no UCO ($n = 12$). Within each experimental group, fetuses were assigned to receive hu-BM-MSCs, human recombinant G-CSF or a sham treatment (saline) (figure 2). All procedures were performed in accordance with the Animal Ethics Research Committee of Maastricht University, The Netherlands.

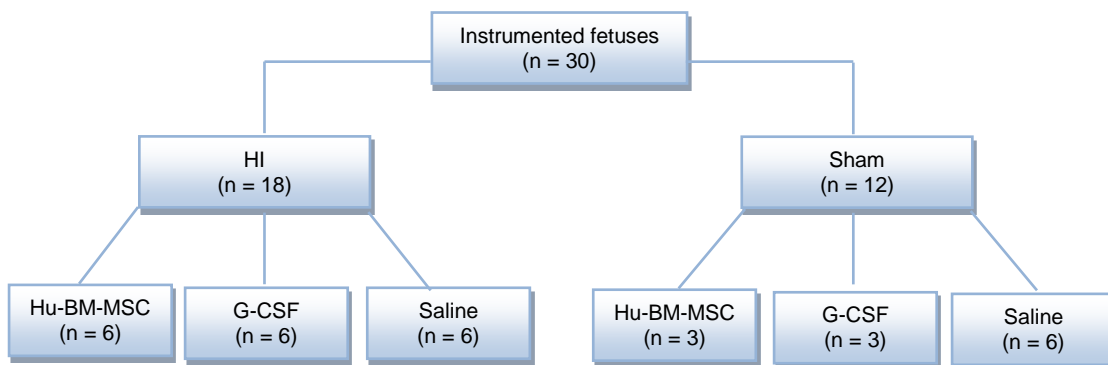


Figure 2: Experimental Groups. Fetal sheep ($n = 30$) with a GA of 102 ± 0.9 (mean \pm SD) days were randomly assigned to receive either UCO ($n = 18$) or sham ($n = 12$). In the HI group, fetuses were assigned to receive hu-BM-MSCs ($n = 6$), G-CSF ($n = 6$) or a sham treatment (saline) ($n = 6$). Each experimental group was controlled by a non-HI group ($n = 12$) that received the same treatment.

2.2 Experimental design

Ewes received intravenous (i.v.) prophylactic antibiotics (1000 mg amoxicillin and 200 mg clavulanic acid) before the surgical procedure. Anesthesia was induced by thiopental (i.v., 15 mg/kg). Following intubation, general anesthesia was maintained with 1-2% isoflurane guided by depth of sedation and supplemented by remifentanyl i.v. (0.75 μ g/kg/min) for analgesia. Certified personnel was responsible for the continuous monitoring of sedation depth and vital parameters. A peri-operative saline drip (250 mL/ hour) was provided by a catheter positioned in the maternal long saphenous vein. The same access was used for post-operative blood sampling and the administration of prophylactic antibiotics for four days. French polyurethane umbilical vessel catheters (Tyco Healthcare Group, Mansfield, Massachusetts, USA) were placed in the femoral artery and brachial vein of the fetus. Fetal heart rate recordings were achieved by three custom-made electrocardiogram (ECG) shielded electrodes (Cooner wire Co., Chatsworth, CA, USA) with silver plates that were sewn on the chest. Two pairs of custom-made electroencephalogram (EEG) shielded electrodes (Cooner wire Co., Chatsworth, CA, USA) with silver tips were placed bilaterally on the dura over the parasagittal parietal cortex (5 mm, 15 mm and 10 mm lateral), with a reference electrode sewn over the occiput. Cyanoacrylate glue was used to secure the EEG electrodes and to close the skin over the fetal skull. An inflatable silicone vascular occluder (OC16HD, 16mm, In Vivo Metric, Healdsburg, California, USA) was placed around

the umbilical cord of all fetuses. Amniotic pressure was recorded via a catheter present in the amniotic sac. Before closure of the uterus, 80 mg of Gentamycin was administered into the amniotic sac. All fetal catheters and leads exited the ewe's flank through a trocar hole and were connected to perfusion pumps for continuous heparinized saline infusion (25 IU/ mL, 0.2 mL/hour). Ewes were housed in confined spaces to allow handling and daily inspection of the surgical wounds, which were treated with chlortetra spray to prevent infection. Animals had *ad libitum* access to water and food and welfare was daily verified by certified personnel. At a GA of 106 ± 0.9 days (mean ± SD) assigned fetuses were subjected to 25 minutes of UCO by inflating the vascular occluder with saline. This was accompanied by close monitoring of vital parameters (blood pressure, EEG and ECG) using the MPAQ system (IDEEQ, Maastricht Instruments). Complete occlusion was confirmed with a sudden drop in heart rate, reduced amplitude of the EEG and arterial blood gas analysis indicating acidemia, hypoxia and hypercapnia. Occlusion was stopped earlier when the mean arterial pressure dropped below 8 mmHg or when asystole occurred. During the seven-day reperfusion phase, sheep fetuses received either hu-BM-MSC (2.0×10^6 cells/kg fetal body weight suspended in 1 mL PBS), human recombinant G-CSF (100 µg/kg fetal body weight) or saline (0.9%). In the hu-BM-MSC experimental group, stem cells were administered within one hour following UCO while G-CSF therapy was started one day before the onset of UCO and continued for five consecutive days. This treatment regimen was chosen to assure the presence of mobilized endogenous stem cells within the therapeutic window of opportunity (few hours after UCO) (figure 3).

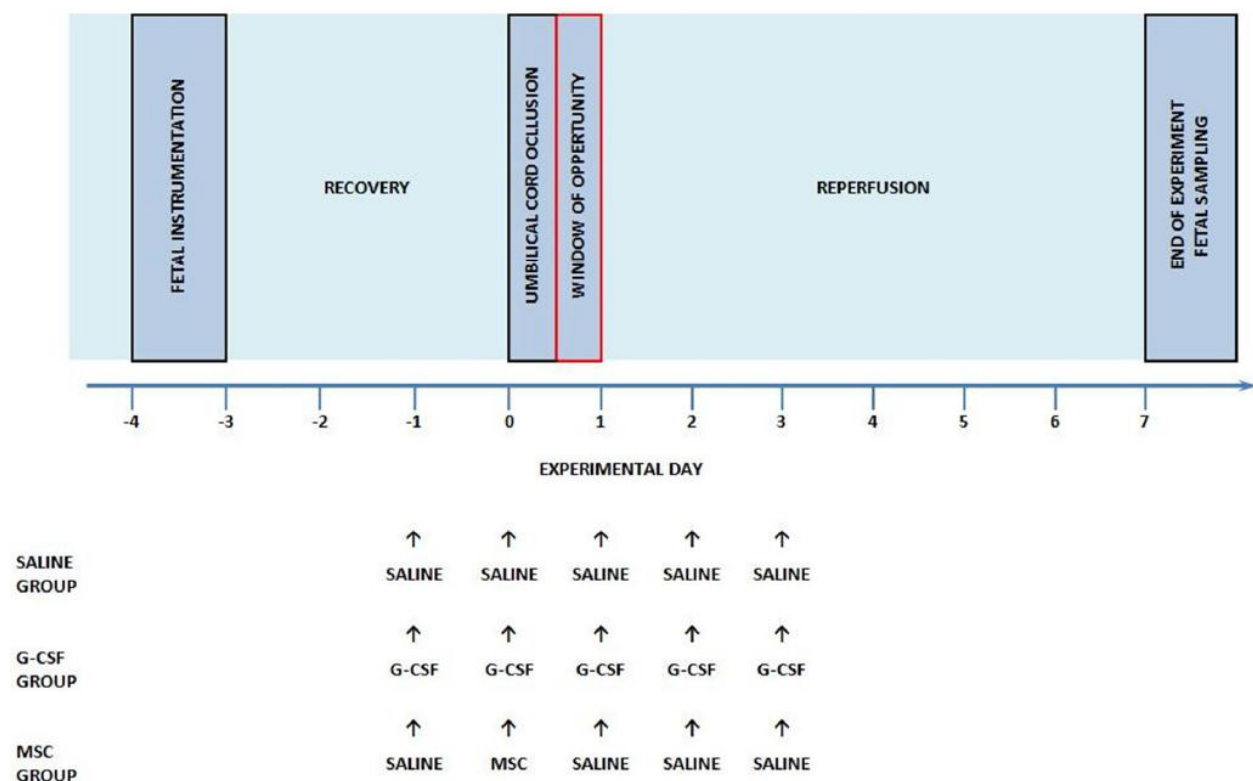


Figure 3: Experimental set-up. Texel fetal sheep (n = 30) were instrumented at 102 days of gestation (term = 145 days) (experimental day -4). On day 0, part of the fetuses (n = 18) underwent a global HI insult by means of UCO. All fetal sheep received either hu-BM-MSCs, human recombinant G-CSF or saline. Following a reperfusion period of seven days, fetuses were humanly euthanized and organs were sampled for analysis.

At experimental day seven, ewe and fetus were humanly euthanized by a lethal dose of pentobarbital (200 mg/kg) and the fetus was delivered immediately. Fetal brains were rapidly removed from the skull, weighed and halved in the mediosagittal plane. At the time of collection, right hemispheres were submersion fixated for three consecutive months by storage in ice-cold paraformaldehyde (4% in 0.1M phosphate buffer).

2.3 Stem cell and G-CSF preparations

Hu-BM-MSCs were purchased from Millipore (Billerica, Massachusetts, USA) and processed according to the manufacturer's instructions. Following four passages, cells were frozen in freezing medium containing 10% Fetal Calf Serum (FCS) and 10% Dimethyl Sulfoxide (DMSO) and stored in nitrogen. The differentiation capacity of the expanded cells into osteoblasts and adipocytes was checked (data not shown) and MSC phenotype was confirmed by flow cytometry analysis.

Human recombinant G-CSF (960 µg/mL) was a gift from Dr. Gerard Bos (Department of Hematology of Maastricht University Medical Centre). According to the manufacturer's protocol, G-CSF was diluted to a concentration of 200 µg/mL (\pm 100 µg/kg fetal body weight), filled into sterile syringes and stored at 4°C.

2.4 Histology tissue preparation

Brain regions containing the cerebral cortex, underlying white matter, hippocampus and thalamus were excised from the right hemispheres. The first cut was made on the rostral side of the thalamus, perpendicular to the corpus callosum (figure 4A). On the caudal side of the brain, the second cut was made through the pineal body (figure 4B).

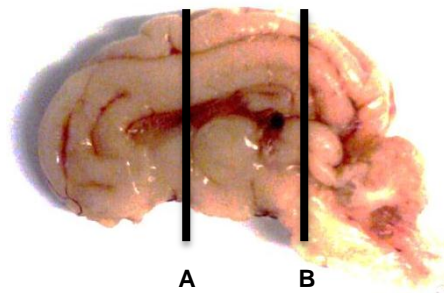


Figure 4: Isolation of the cerebral region of interest. Lines A and B illustrate how right hemispheres were cut on respectively the rostral and caudal side of the fetal sheep brain.

Following the removal of membranes and blood vessels, cerebral regions were embedded in lukewarm gelatin (10% in milliQ) and stored for 2 hours at 4°C. Next, they were put on paraformaldehyde (4% in 0.1M phosphate buffer) for 4 hours at 4°C and preserved in sodium azide (1% in 0.1M phosphate buffer). Evenly spaced coronal sections (50 µm) of the forebrain were cut on a vibrating microtome (Leica VT 1200S; Leica Biosystems Nussloch, Germany). The hippocampus was found in 5-8 sections per subseries, depending on its individual rostrocaudal extension. The left hemispheres were not used in the present study.

2.5 Area estimates

For estimations of numerical densities, areas of the dorsal level of the hippocampus were determined prior to analysis. High-resolution digital images of synaptophysin stained sections were obtained using an Olympus BX51 microscope (Olympus, Tokyo, Japan) equipped with a motorized stage and a digital camera. Single images, initially acquired during the scanning process at 2X magnification, were automatically stitched together to generate a virtual overview image of the entire slide. Virtual Slide software was used to select the region of interest and integrated focus routines made sure that the image was always in focus. Virtual Slide Images (VSI) at 10X magnification were exported and converted to JPEG format using OlyVIA software (Olympus, OlyVIA 2.4, XV 3.5) and Photoshop CS4 (Adobe Photoshop CS4 extended version 11.0). Area measurements were performed with Leica QWin software (Leica Qwin Pro V 3.5.1, Switzerland) by delineating the dorsal level of the hippocampus. Results were displayed in a specialized program designed by J. Cleutjens (Department of Pathology, Maastricht University Medical Centre).

2.6 Nissl staining

One series of sections was mounted on glass slides and dried overnight. Sections were defatted with a Triton-X100 solution, stained with cresyl violet (0.01%) for 25 minutes and coverslipped with DePex. Nissl stained sections were used to demonstrate nuclear and cytoplasmic RNA (Nissl-substance). Neuronal stratification patterns were determined in the following hippocampal regions: Cornu Ammonis (CA)1-2, CA3 and Dentate Gyrus (DG).

2.7 Immunohistochemistry

Immunohistochemical stainings were performed on sections at the level of the mid-thalamus and hippocampus. Six sections per animal were selected for the detection of presynaptic boutons, microglia or pre-oligodendrocytes. All stainings were carried out in a free-floating manner. Sections were processed simultaneously to guarantee identical conditions. With exception of the pre-oligodendrocyte staining, all washing steps were done by using alternately Tris-Buffered Saline (TBS; 0.05M, pH 7.6) or Tris-Buffered Saline Triton (TBS-T; 0.05M TBS with 0.2% Triton-X-100) at room temperature. In order to deactivate endogenous peroxidase activity, sections were pre-incubated with H₂O₂ (0.3% in TBS) for 30 minutes.

Synaptophysin is an integral membrane protein located in presynaptic vesicles and therefore a good marker to detect nerve terminals. Sections were incubated overnight with the anti-synaptophysin primary antibody (monoclonal mouse, 1:2000 in 0.3% donkey serum; Millipore, Massachusetts, USA) at 4-8°C, where after they were sequentially incubated with donkey anti-mouse biotinylated secondary antibody (1:400 in 0.3% donkey serum, Bio-Connect) for 1.5 hour at room temperature.

Ionized calcium-binding adaptor molecule 1 (IBA-1) is specifically expressed on microglia in the brain. An anti-IBA-1 antibody (monoclonal rabbit, Abcam, Cambridge, England) was used as primary antibody overnight at a dilution of 1:200 at 4-8°C, followed by immersion with a donkey-anti-rabbit biotinylated secondary antibody (1:200, Bio-Connect, The Netherlands) for 2 hours at room temperature.

The presence of pre-oligodendrocytes in the CNS was determined in sections immunohistochemically stained for O4 (monoclonal mouse, 1:400; Millipore, Massachusetts, USA), which is expressed on the cell surfaces. Following a primary antibody incubation of 3 days at 4-8°C, sections were incubated with a donkey anti-mouse biotinylated secondary antibody (1:400, Bio-Connect, The Netherlands) for 1.5 hour at room temperature.

All sections were further processed using the avidin biotin complex technique with 3,3-diaminobenzidine (DAB) to obtain a color reaction. Nickel chloride (8%) enhancement was used in both O4 and IBA-1 stainings. Following the labeling procedures, sections were mounted on gelatin-coated glass slides, air-dried, dehydrated in ascending ethanol concentrations and cover slipped with PerTex.

2.8 Neuropathological examination

2.8.1 Quantitative analysis of synaptophysin staining

Presynaptic bouton densities were analyzed in the following hippocampal regions: stratum radiatum (SR) of area CA1-2, stratum lucidum (SL) of area CA3 and stratum moleculare (SM) of DG (figure 4). A digital camera (F-view; Olympus, Tokyo, Japan) attached to an Olympus AX-70 microscope (Olympus, Tokyo, Japan) was used to take two (CA3) to three (CA1-2 and DG) high-resolution photographs at 40X magnification. Four to six different sections of each animal were analyzed in the aforementioned areas, yielding 32 to 48 photos for each animal.

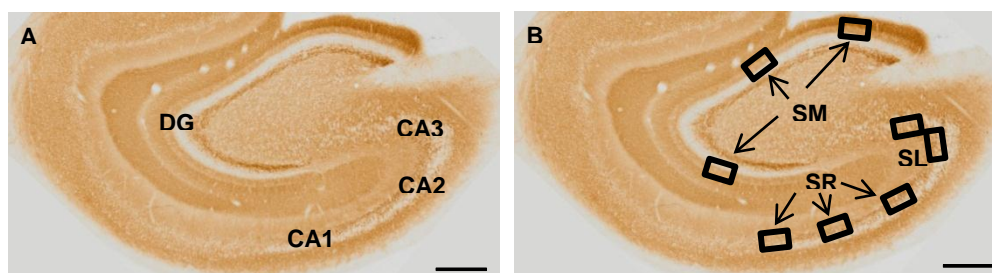


Figure 5: Representative photomicrograph of a frontal section through the hippocampal formation of a control fetus. Synaptophysin immunoreactivity is present in the following hippocampal regions: CA1-2, CA3 and DG (A). The squares in figure B represent the areas where the photomicrographs for quantitative analysis were taken within the SM, SL, and SR. CA: cornu ammonis, DG: dentate gyrus, SM: stratum moleculare, SL: stratum lucidum, SR: stratum radiatum. Scale bar = 500 μ m.

Using the Cell-P image analysis system (Soft Imaging System, Münster, Germany), synaptophysin immunoreactive punctae were detected in a single focal plane. Prior to picture analysis, background levels were equalized using a DCE filter and a shading error correction was performed in order to correct for irregularities in illumination of the microscopic field. Threshold values providing the most accurate measurement compared to direct visual counting were selected and were kept the same for all photographs.

2.8.2 Calculation of the presynaptic bouton density

Hippocampal region-specific presynaptic bouton density was calculated by dividing the individual density data with the area of the corresponding hippocampus.

2.8.3 Quantitative analysis of IBA-1 staining

VSI at 10X magnification of IBA-1 stained sections were made as described in section 2.5. Using Leica Qwin software (Leica Qwin Pro V 3.5.1, Switzerland), microglial density was determined in the total hippocampus, in CA1-2, CA3 and DG separately and in the PVWM. Four to six different sections of each animal were analyzed in the aforementioned areas. The CA2 hippocampal region was not separated from CA1 and CA3 since it was difficult to demarcate this region based on IBA-1 immunohistochemistry. A straight line that linked the beginning of the SL and the tip of the suprapyramidal blade of the DG indicated the border between the CA1-2 and CA3 (60). A standard region that was sampled in all images was determined by a line drawn from the midpoint of the insular lobe, perpendicular to the lateral ventricle. Thresholds for cell detection were tested in advance by using the trial and error method and were kept the same for all photographs. Blood vessels and tissue out of focus were excluded.

2.8.4 Quantitative analysis of O4 staining

VSI at 10X magnification of O4 stained sections were made as described in section 2.5. The total density of O4-labeled cells in PVWM was determined in four to six adjacent serial sections per experimental animal. The PVWM was defined as the region bounded by the lateral aspects of the lateral ventricle. A standard region that was sampled in all images was determined by a line through the PVWM drawn perpendicular to the dorsal part of the hippocampus (figure 6). Intact appearing as well as degenerating pre-oligodendrocytes were counted in a blinded manner using a counting frame with a predefined size. In order to avoid potential “edge artifacts”, fields adjacent to tissue edges or blood vessel were not used in cell counting.

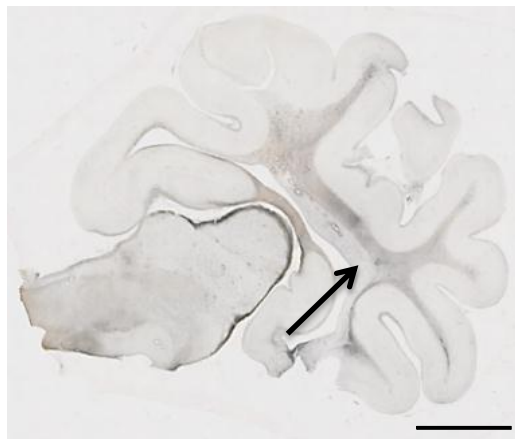


Figure 6: Representative photomicrograph of a coronal section, stained for O4, through the right hemisphere of a control fetus (A). The strong O4 staining pattern in white matter tracts is illustrated. Pre-oligodendrocytes present in the PVWM were counted in a blinded manner using a counting frame with a predefined size. Scale bar = 5 mm.

2.9 Statistical analysis

Statistical analysis and graphical presentation was performed with PASW Statistics 18 (SPSS Inc., Chicago, IL, USA). Values between experimental groups were compared using Mann-Whitney U test with Bonferroni post-hoc correction where appropriate. A p-value of ≤ 0.05 was used to denote statistical significance.

3. Results

3.1 Baseline characteristics

All fetuses had normal blood gasses, heart rate and mean arterial blood pressure before each experiment, according to the standards of our laboratory. UCO led to hypotension, bradycardia, acidosis, hypoxemia and hypercapnia. Reperfusion was associated with a rapid recovery of all parameters (Figure 7 A - E).

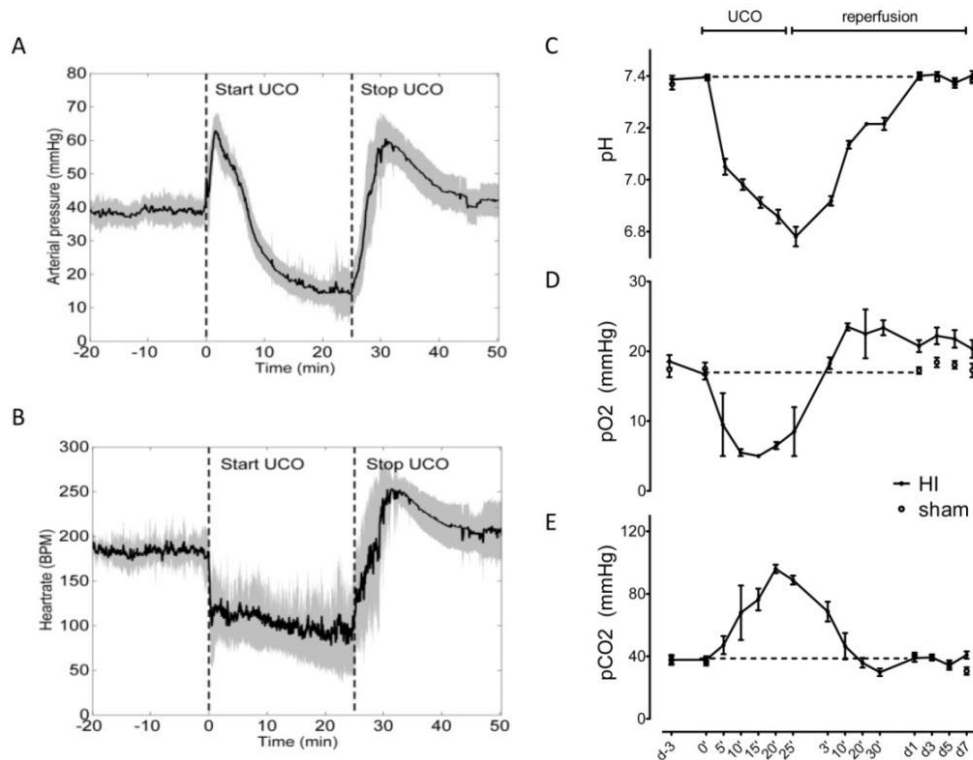


Figure 7: Vital parameters and blood gases during UCO. HI episodes were accompanied by hypotension (A) bradycardia (B) acidosis (C) hypoxemia (D) and hypercapnia (E). Release of the umbilical occluder was associated with a rapid recovery of all parameters.

Fetal instrumentation was performed on a standardized GA (GA = 0.7). Global HI appeared not to have an effect on fetal body weight (Table 1).

Table 1: GA (days) at UCO and fetal body weight (g). Fetal instrumentation was performed on a standardized GA (GA = 0.7). No differences in body weight were detected between the sham and the HI group.

	GA at UCO		BW (g)	
	mean	SEM	mean	SEM
sham-SAL	105.50	0.34	1791.92	78.93
sham-MSC	105.33	0.29	1783.00	68.19
sham-G-CSF	105.67	0.33	1819.67	128.29
HI-SAL	105.31	0.31	1742.00	114.89
HI-MSC	106.14	0.46	1981.14	185.24
HI-G-CSF	105.71	0.18	1764.29	125.11

3.2 Objective 1: hypoxic-ischemic damage to the preterm brain

3.2.1 Brain weight

Figure 8 illustrates the effect of global HI on brain weight. Compared to the sham control group, the cerebral weight of occluded animals was significantly decreased ($p=0.001$).

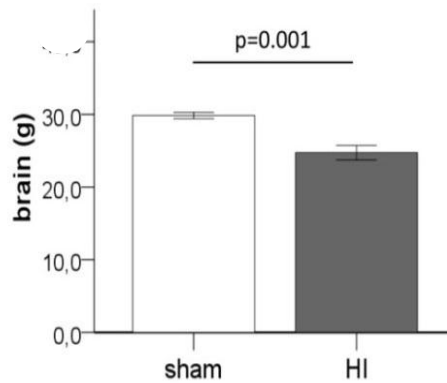


Figure 8: Cerebral weight (g) significantly decreased after global HI. $P = 0.001$.

3.2.2 Hippocampal atrophy

Analysis of the fetal hippocampus showed profound atrophy after UCO (Figure 9A; $p<0.001$). Results from individual hippocampal regions demonstrated that the Ammon's horn was the most affected (CA1-2; $p<0.001$ and CA3; $p=0.001$), while the DG area was rather preserved ($p=0.037$) (Figure 9 B - D).

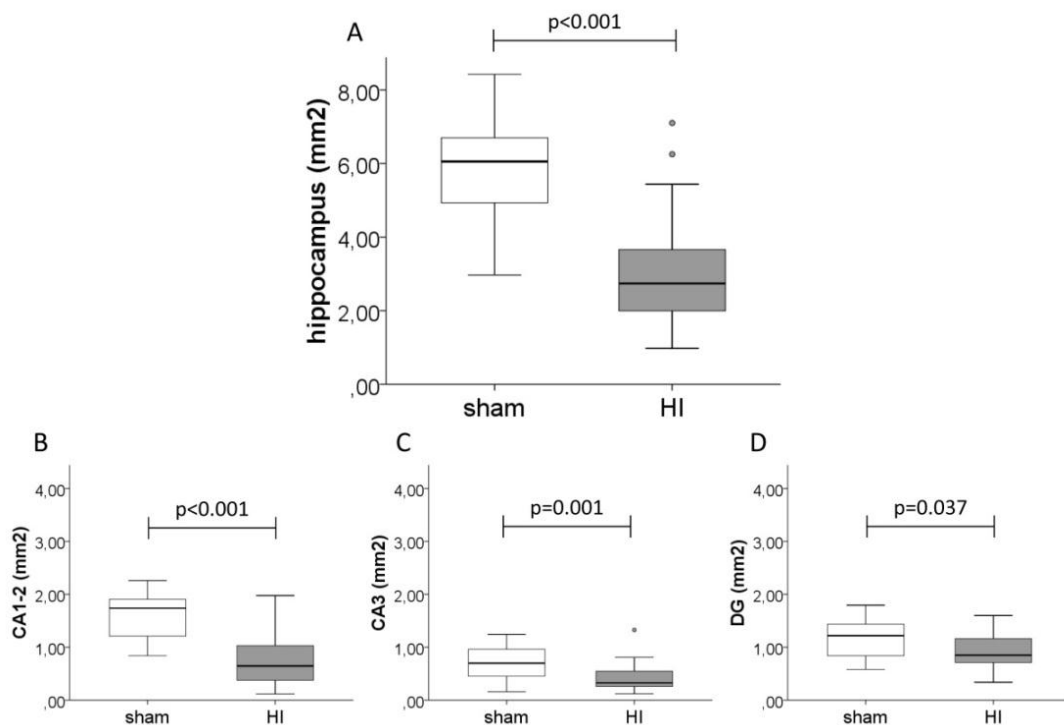


Figure 9: Area (mm²) of the total hippocampus and individual hippocampal regions. Following global HI, a significant decrease in total hippocampal area was observed ($p<0.001$). Results obtained per hippocampal region demonstrated that atrophy was present in all areas (CA1-2: $p<0.001$; CA3: $p=0.001$ and DG: $p=0.037$).

3.2.3 Presynaptic bouton density

The effects of global HI on presynaptic bouton densities in the SR of CA1-2, the SL of CA3 and the SM of the DG are shown in figure 10 (A - F). Graphs A to C depict the results of presynaptic bouton densities without hippocampal area correction in CA1-2, CA3 and DG respectively. With exception of CA1-2 ($p=0.014$), no overall differences were observed between both groups. Taking the area measurements into account, analysis demonstrated an overall effect of group on bouton density as all hippocampal regions in the HI group showed values that were significantly higher when compared to control animals (CA1-2; $p<0.001$, CA3; $p=0.001$, DG; $p<0.001$).

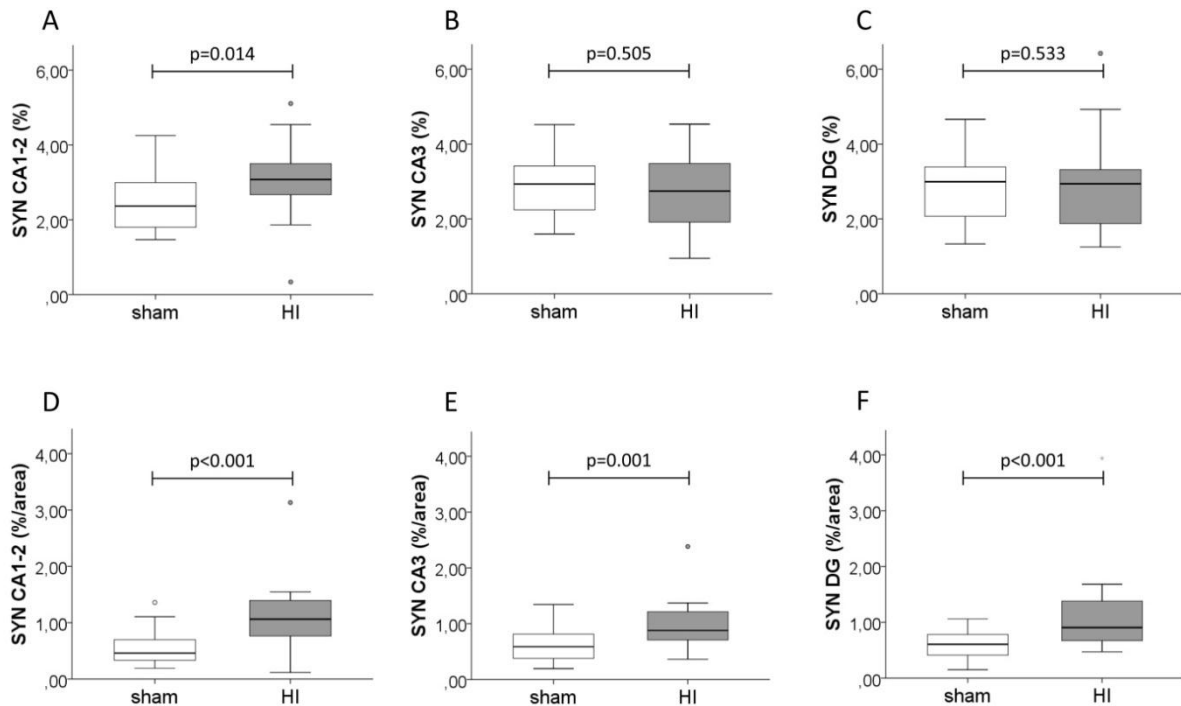


Figure 10: The area fraction (%) of synaptophysin staining (A – C) and the area fraction (%) corrected for the area of the hippocampus (D - F). After correcting for hippocampal area, significant increases in presynaptic bouton density were observed in all hippocampal regions of occluded animals.

Morphology data showed that synaptophysin staining was uniformly strong. Immunoreactivity was restricted to small punctae, representing presynaptic boutons (figure 11).

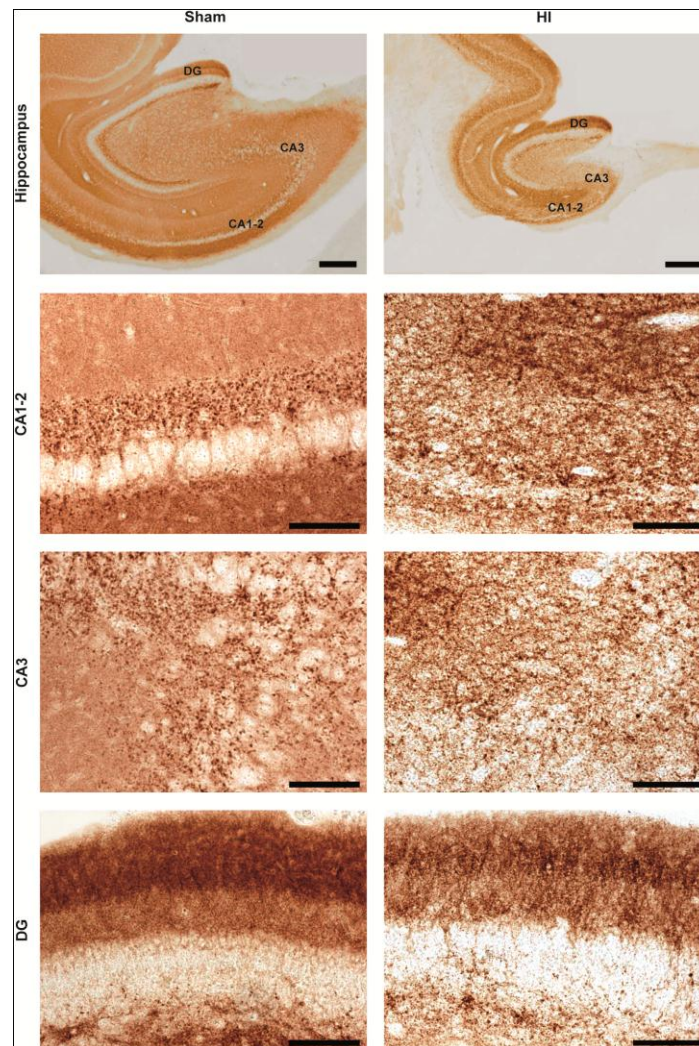


Figure 11: Photomicrograph of synaptophysin staining in the SR of CA1, the SL of CA3 and the SM of DG of sham-control animals and fetal sheep subjected to global HI. Pictures show an increased and a more diffuse synaptophysin immunoreactivity following a global HI insult. The strata of the DG show an increased staining pattern. Scale bar hippocampus: 500 μ m. Scale bar CA1-2, CA3 and DG: 100 μ m.

As depicted in figure 11, the CA1-2 and CA3 regions of sham animals showed a strong staining pattern in and around the neuronal cell bodies while leaving the perikarya free of staining. Global HI was not associated with perceptible loss of synaptophysin immunoreactivity. Presynaptic bouton density was more diffuse in the occluded group and the sharp demarcation at gray-white junctions was lost. In addition, strata of the DG were preserved and showed a stronger staining pattern.

3.2.4 Neurons

Analysis of the hippocampal formation revealed that systemic HI insult was accompanied with gross changes in hippocampal structure and morphology.

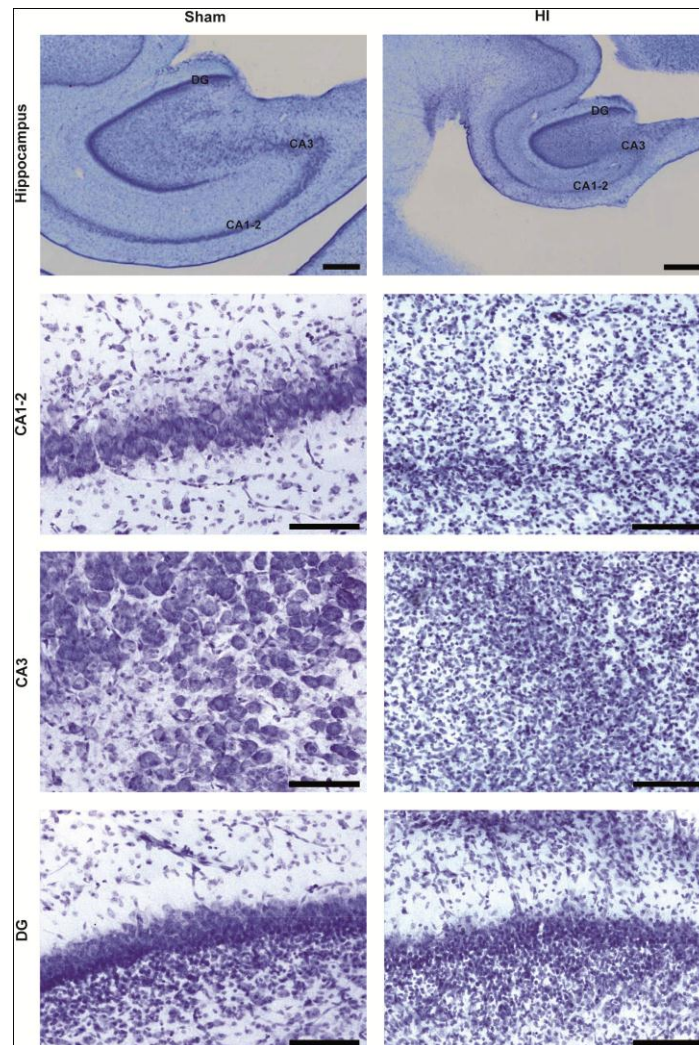


Figure 12: Nissl staining showing the SP of CA1-2 and CA3 and in the SG of the DG in sham and occluded fetal sheep. Note the compact SP in CA1-2 and CA3 of sham control animals and the loss of pyramidal cells in the Ammon's horn following HI. SP: stratum pyramidale, SG: stratum granulosum. Scale bar hippocampus: 500 μ m. Scale bar CA1-2, CA3 and DG: 100 μ m.

Cytoarchitectural investigations on neuronal density, size and shape in the fetal hippocampus were performed using the conventional staining of the Nissl substance with cresyl violet. Staining produced the expected appearance with visualization of neurons and glia. It is eminent that the CA1-2 and CA3 regions of occluded animals had an altered neuronal density in comparison to controls. Excitatory pyramidal cells in CA1-2 were more compact in sham animals whereas a more scattered stratum pyramidale with shrunken neurons was observed in CA1-2 of fetal sheep subjected to HI. Similar observations were made in CA3. In addition, HI was accompanied by chromatolysis of CA1-2 and CA3 pyramidal cells. Neurons of the stratum granulosum (SG), however, showed less ultrastructural changes following global HI as the demarcation between the different strata in the DG was still present. Furthermore, a general increase in cell density was observed in the hippocampus of fetal sheep subjected to systemic HI.

3.2.5 Microglial density in the hippocampus

Our results show that a global HI insult, followed by a reperfusion period of 7 days, was accompanied by a significant increase in microglial reactivity in the fetal hippocampus. This was demonstrated by an increased microglial density (Figure 13) and changes in cell morphology (Figure 14). In the Ammon's horn, the density of IBA-1 positive cells was significantly increased to similar levels (CA1-2 and CA3: $p < 0.001$). Although significant, less microglial expansion was observed in the DG ($p < 0.001$).

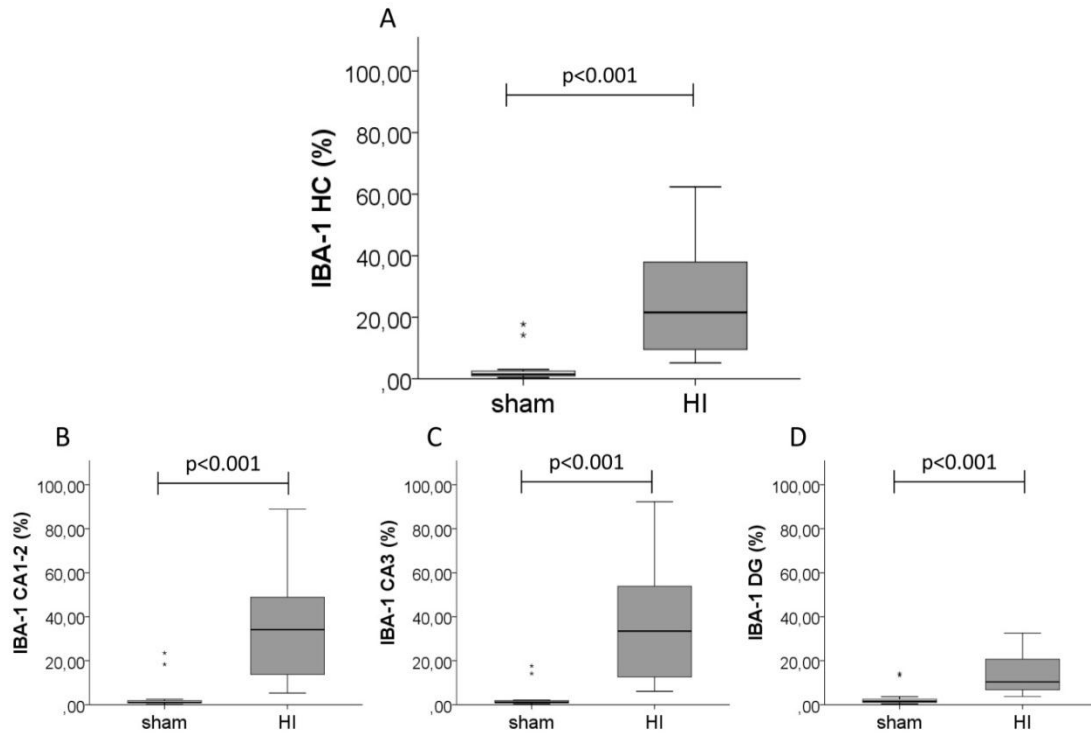


Figure 13: Densitometric analysis (%) of IBA-1 expression in the hippocampus of sham-control and occluded fetal sheep. Results demonstrate profound microglial proliferation in all hippocampal areas of animals subjected to systemic HI ($p < 0.001$ in all areas). HC: hippocampus.

Hippocampi of both experimental groups demonstrated a homogeneous microglial distribution pattern in the Ammon's, while a lower microglial density was observed in the DG. Furthermore, morphological changes of microglia from the resting to the activated state were detected. Hippocampi of sham animals showed resting microglia with compact cell bodies and branched processes. Though, in some brains we encountered a few IBA-1 positive cells with a different shape, i.e. larger somata with intensely labeled processes (results not shown). In contrast, activated microglia with prominent cell bodies and short, tick processes were present in all hippocampal regions of fetal sheep subjected to global HI.

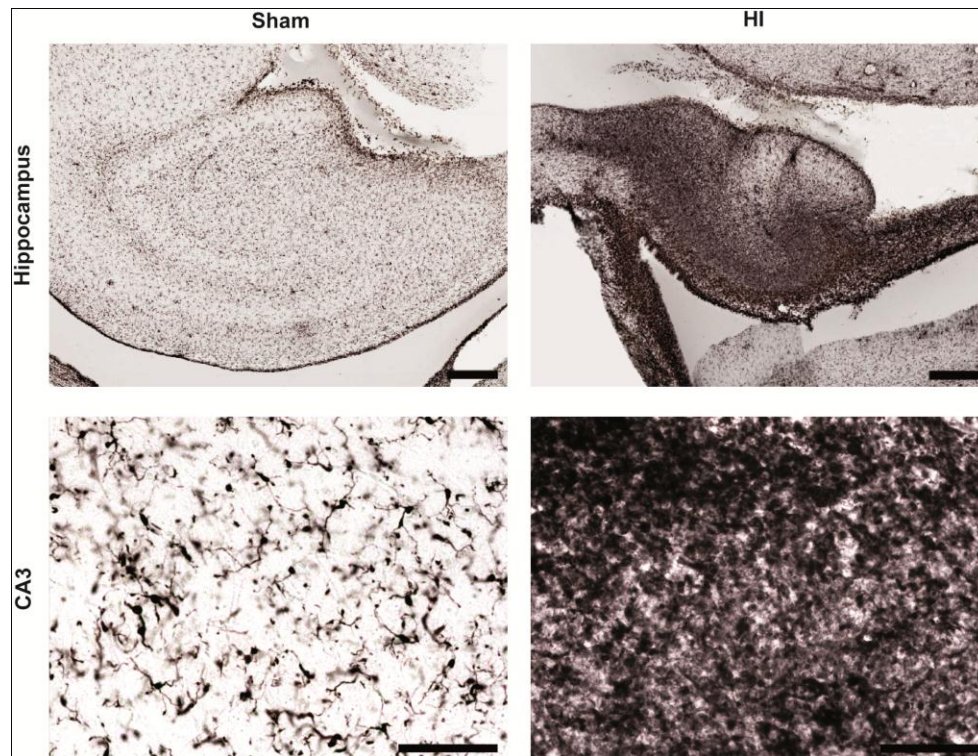


Figure 14: Photomicrograph showing microglial proliferation and activation in a representative sham and occluded animal. Microglia were scattered throughout the hippocampus. IBA-1 immunohistochemistry revealed profound microglial proliferation after HI. Moreover, a progression from resting microglial cells in the sham group to microglial activation in the HI group was shown in the CA3 region of the hippocampus. Scale bar hippocampus = 500 μm . Scale bar CA3 = 100 μm .

3.2.6 Microglial density in the periventricular white matter

Compared to the sham control group, systemic HI was associated with an increased density of IBA-1 labeled cells (Figure 15, $p < 0.008$).

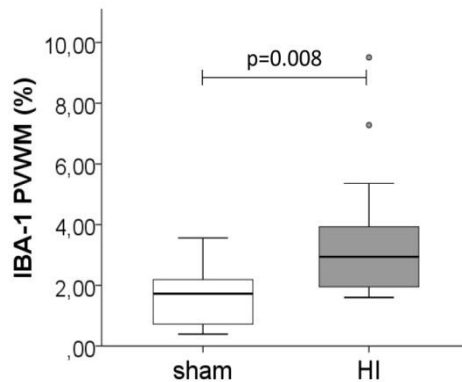


Figure 15: Quantitative analysis of microglial density (%) in the PVWM of sham and occluded fetal sheep. HI was associated with a significant increase in microglial density in the PVWM.

Morphology data illustrate the typical ramified morphology of resting microglia in the PVWM of the sham-control group. Following global HI, both an increase in microglial density and a shift from a resting to an activated cellular state were observed (figure 16).

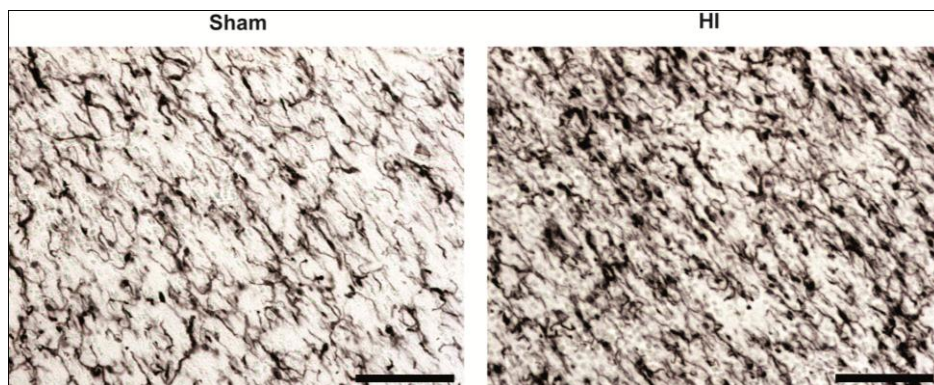


Figure 16: Histopathological features of the PVWM as visualized by IBA-1 immunohistochemistry. An increased microglial density and activated cells were detected in the PVWM of animals exposed to global HI. Scale bar = 100 μ m.

3.2.7 White matter O4 expression

Pre-oligodendrocyte numbers were monitored in a predefined area of the PVWM. A dense O4-positive staining was observed in the sham-control group, while the PVWM of the HI group showed a significant loss of O4-positive cells (Figure 17; $p < 0.001$).

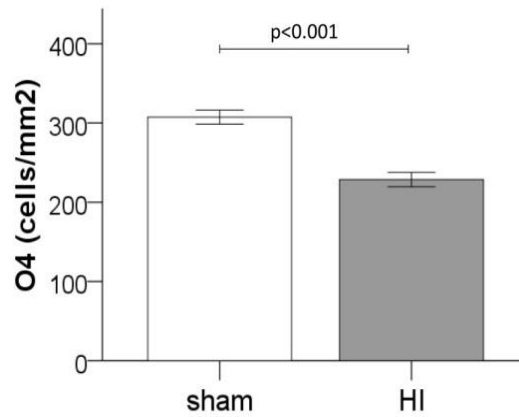


Figure 17: Number of O4 immunopositive cells/mm² in a predefined area of the PVWM. Global HI was accompanied by a significant reduction in the number of pre-oligodendrocytes ($p < 0.001$).

Pre-oligodendrocytes in the sham-control and the HI group were morphologically diverse (figure 17). In control PVWM, cells displayed a complex multipolar morphology characterized by a round soma that elaborated numerous extensively branched processes. Pre-oligodendrocytes in the PVWM of the occluded group had a more simple, morphologically less mature, appearance.

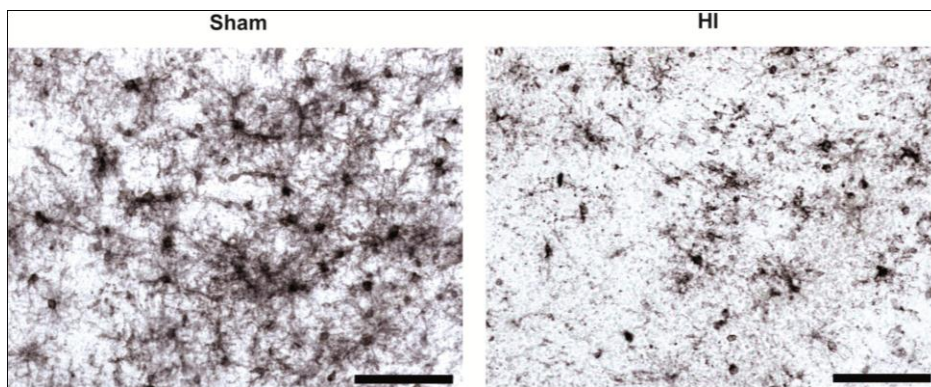


Figure 18: Pre-oligodendrocytes in the PVWM of the sham-control group and the occluded animals. O4 immunohistochemistry revealed a morphologically dense staining in the PVWM of control animals while the pre-oligodendrocyte number was significantly decreased following HI. Moreover, pre-oligodendrocytes in the PVWM of animals subjected to global HI displayed cells with a morphologically immature appearance. Scale bar = 100 μ m.

3.3 Objective 2: MSC and G-CSF therapies in neonatal hypoxic-ischemic encephalopathy

3.3.1 Brain weight

Cerebral weight did not differ between the sham-SAL, sham-MSC and sham-G-CSF experimental groups. As described in 3.2.1, global HI was accompanied by a significant decrease in brain weight ($p=0.001$). G-CSF administration following UCO did not have therapeutic effects on cerebral weight since significant differences were observed between the sham-SAL and HI-G-CSF experimental groups ($p=0.002$). Administration of exogenous MSCs, however, preserved brain weight. Though, differences between HI-SAL and HI-MSC did not reach the critical level of significance ($p=0.362$), indicating only minor therapeutic effects of MSCs on cerebral weight (figure 19).

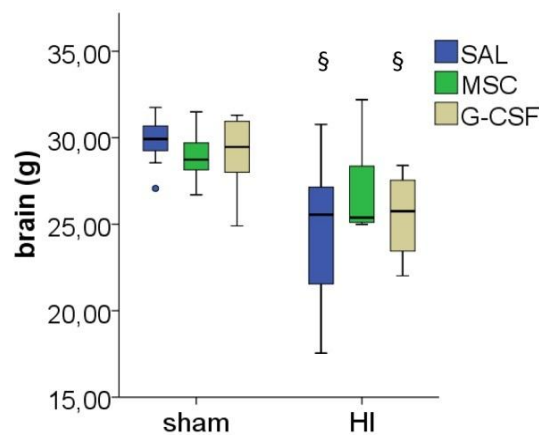


Figure 19: Cerebral weight (g) for all experimental groups. Brain weight significantly decreased following global HI. MSC administration after UCO was associated with brain weight recovery towards control values. No significant differences were observed between HI-SAL and HI-MSC experimental groups, indicating only minor influences of MSC therapy on brain weight recovery. Administration of G-CSF following UCO did not influence cerebral weight.

Table 2: Comparison of brain weight (g) with Mann-Whitney U test and Bonferroni correction. P-values of comparisons for cerebral weight are shown. § $p<0.01$ (compared to sham-SAL).

	<u>brain (g)</u>
sham-SAL vs. HI-SAL	0.001*
sham-SAL vs. HI-MSC	0.057
sham-SAL vs. HI-G-CSF	0.002*
HI-SAL vs. HI-MSC	0.362
HI-SAL vs. HI-G-CSF	0.552
* $p<0.01$ (Bonferroni correction: level of significance: $0.05/5 = 0.01$)	
§ $p<0.05$	

3.3.2 Hippocampal atrophy

Results demonstrate profound atrophy of the hippocampal formation after a systemic HI insult. Additional results show that hippocampal shrinkage was uniform in all occluded groups, representing no therapeutic effects of MSC or G-CSF administration on overall hippocampal area. Data from individual regions revealed no influence of treatment on the CA1-2 and CA3 area of sheep subjected to HI. Contradictory to the Ammon's horn, UCO had no significant effect on the area of the DG ($p=0.037$). When compared to sham-SAL, the G-CSF-occlusion group displayed a significant reduction in DG area (figure 20).

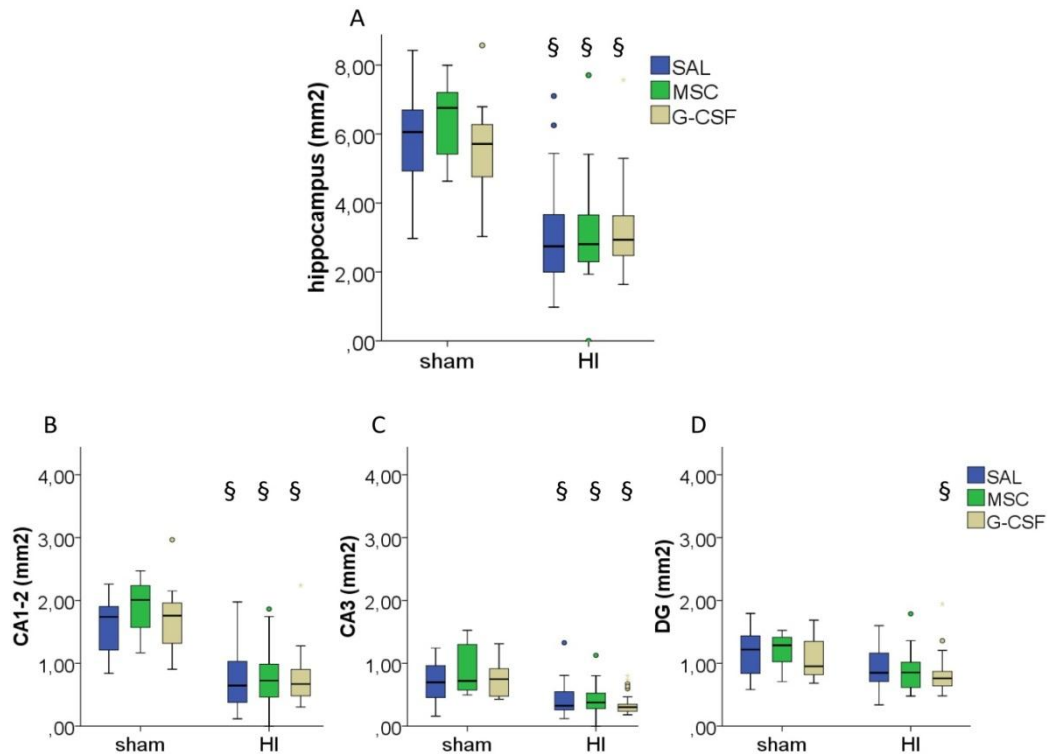


Figure 20: Area (mm²) of the total hippocampus (A) and CA1-2, CA3 and DG (B – D) for all experimental groups. HI induced profound atrophy of the total hippocampus. With exception of the DG, all hippocampal areas were significantly decreased after HI. MSC or G-CSF administration had no effect on overall hippocampal area, neither on CA1-2 or CA3 individually. Regional results for the DG show area shrinkage in the G-CSF occlusion group. MSC therapy had no influence on DG area. § $p<0.01$ (compared to sham-SAL).

Table 3: Comparison of means of hippocampal area (mm²) with Mann-Whitney U test and Bonferroni correction. P-values of comparisons are shown for the total hippocampus and for all hippocampal regions investigated.

	area (mm ²)			
	HC	CA1-2	CA3	DG
sham-SAL vs. HI-SAL	0.000*	0.000*	0.001*	0.037 [§]
sham-SAL vs. HI-MSC	0.000*	0.000*	0.002*	0.014 [§]
sham-SAL vs. HI-G-CSF	0.000*	0.000*	0.000*	0.001*
HI-SAL vs. HI-MSC	0.669	0.627	0.534	0.631
HI-SAL vs. HI-G-CSF	0.491	0.501	0.414	0.223

* $p<0.01$ (Bonferroni correction: level of significance: $0.05/5 = 0.01$)
[§] $p<0.05$

3.3.3 Presynaptic bouton density

Figure 21 A – C demonstrates the area fraction (%) of synaptophysin staining in all experimental groups without correcting for hippocampal area. In CA1-2, no significant differences were observed between the experimental groups. Similar observations were made in CA3, with exception of the HI-G-CSF experimental group where a significant decrease in area fraction was observed when compared to the sham-SAL group ($p=0.003$). Compared to HI-SAL, area fractions were increased in the DG of the MSC - and G-CSF-occlusion groups (not significant). Presynaptic bouton densities were significantly increased in all hippocampal regions when values were corrected for hippocampal area. Moreover, when compared to HI-SAL, a significant increase in fraction area was observed in the DG of the HI-G-CSF experimental group ($p=0.005$).

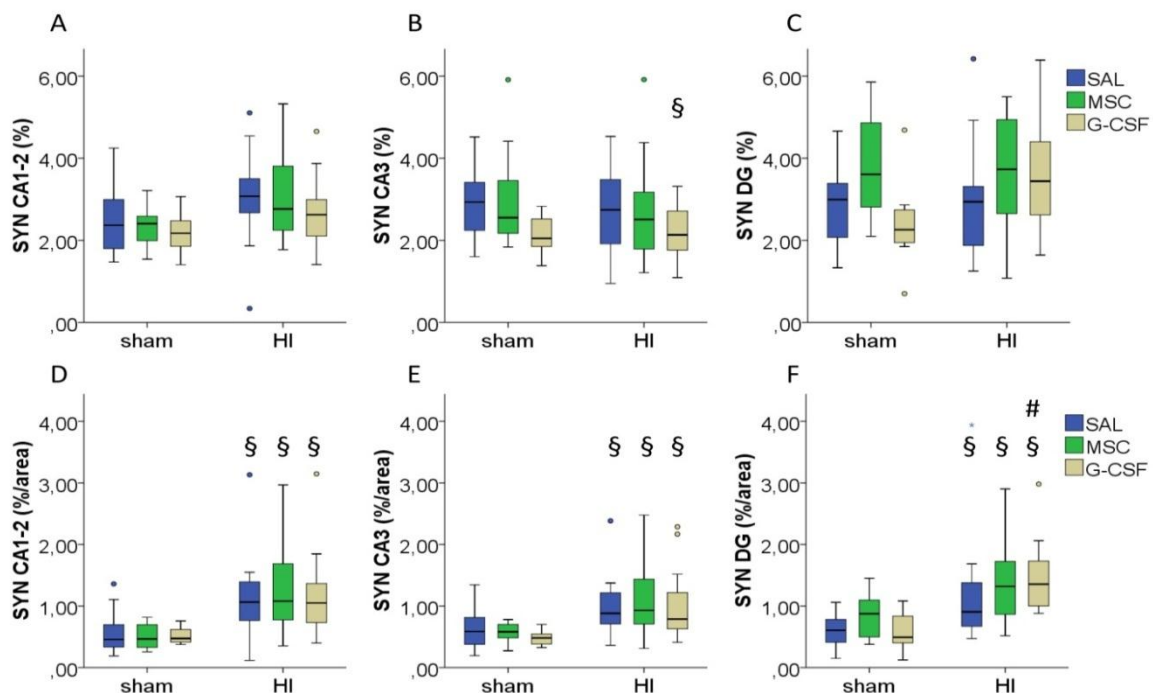


Figure 21: Area fraction (%) of synaptophysin (A-C) and the area fraction corrected for the area of the hippocampus (D-F). § $p<0.01$ (compared to sham-SAL), # $p<0.01$ (compared to HI-SAL).

Table 4: Comparison of means of synaptophysin staining (%) with Mann-Whitney U test and Bonferroni correction. P-values of comparisons are shown for the total hippocampus and CA1-2, CA3 and DG.

	HC (mm ²)	%			%/area		
		CA1-2	CA3	DG	CA1-2	CA3	DG
sham-SAL vs. HI-SAL	0.000*	0.044 [§]	0.505	0.533	0.000*	0.001*	0.000*
sham-SAL vs. HI-MSC	0.000*	0.066	0.204	0.330	0.000*	0.001*	0.000*
sham-SAL vs. HI-G-CSF	0.000*	0.252	0.003*	0.033 [§]	0.000*	0.003*	0.000*
HI-SAL vs. HI-MSC	0.895	0.564	0.646	0.024 [§]	0.832	0.725	0.086
HI-SAL vs. HI-G-CSF	0.722	0.048 [§]	0.082	0.023 [§]	0.845	0.546	0.005*

* $p<0.01$ (Bonferroni correction: level of significance: $0.05/5 = 0.01$)
[§] $p<0.05$

In the hippocampus of sham animals, a strong synaptophysin staining pattern was observed in and around the SP of the Ammon's horn. In addition, the different strata of the DG were sharply demarcated. In the HI-SAL group, CA1-2 and CA3 were characterized by a scattered synaptophysin immunoreactivity. The DG seemed less affected by global HI as the sharp demarcation between gray-white junctions could still be observed. MSC and G-CSF administration after UCO was associated with ultrastructural repair in all hippocampal regions (figure 22).

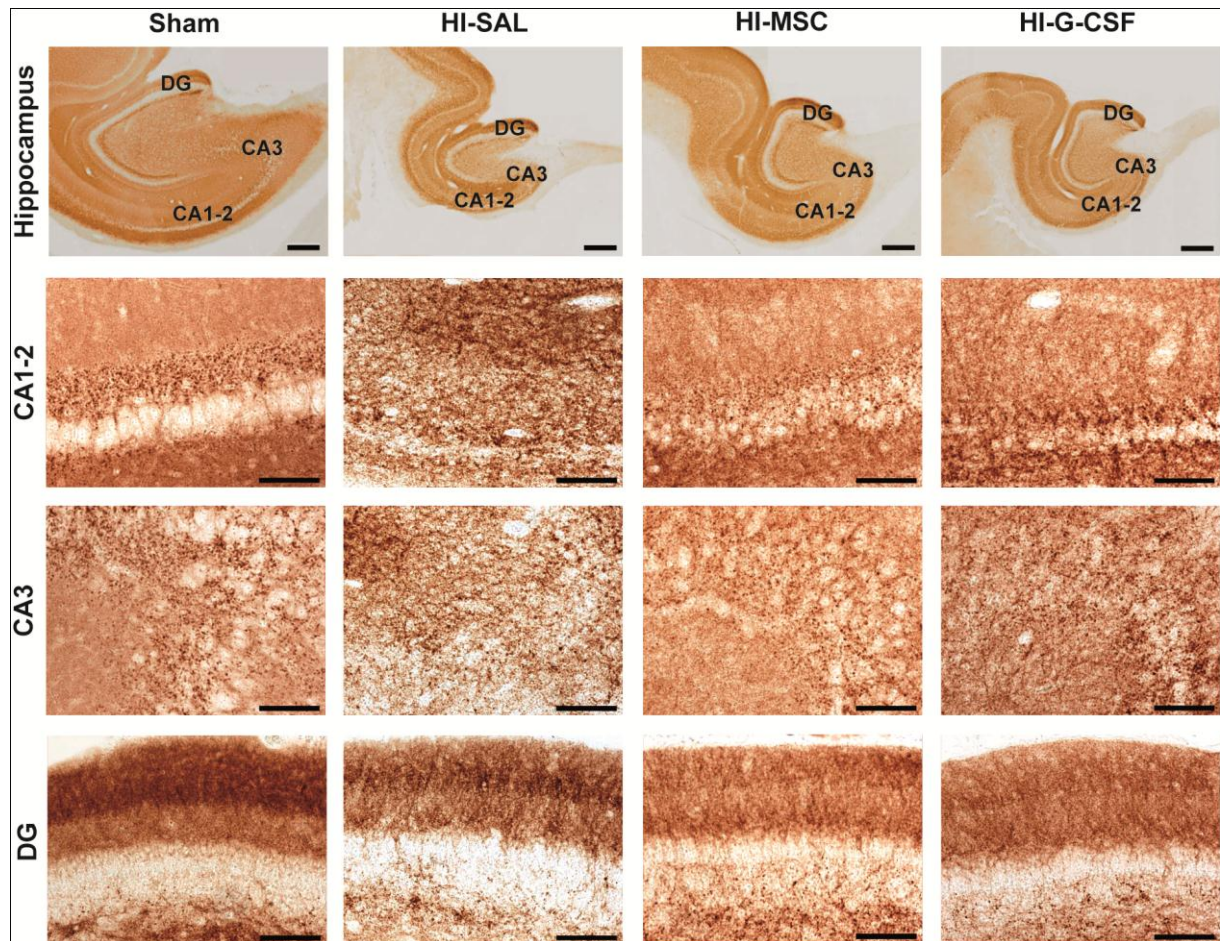


Figure 22: Photomicrographs of synaptophysin staining in the SR of CA1-2, the SL of CA3 and the SM of the DG in a representative sham animal and in the HI-SAL, HI-MSC and HI-G-CSF experimental groups. Global HI was associated with a scattered synaptophysin immunoreactivity in CA1-2 and CA3. The DG appeared to be an area that sustained less damage following HI. In the HI-MSC and HI-G-CSF groups, clear trends towards ultrastructural repair were observed. Scale bar hippocampus: 500 μm . Scale bar CA1-2, CA3 and DG: 100 μm .

3.3.4 Neurons

Nissl staining of representative hippocampi in the sham, HI-SAL, HI-MSC and HI-G-CSF experimental groups (figure 23). Global HI was accompanied with loss of Nissl substance. The SP in CA1-2 and CA3 showed a dark dotted staining, referring to neurodegeneration. Note the compact cell layer of the SP in the Ammon's horn of sham animals relative to the SP in the HI-SAL and the HI-G-CSF groups. Moreover, apparent loss of pyramidal cells in CA1-2 and CA3 was observed in all occluded groups. All hippocampal areas of occluded animals that received MSC showed a clear trend towards ultrastructural repair. Observations were less clear in the G-CSF experimental group.

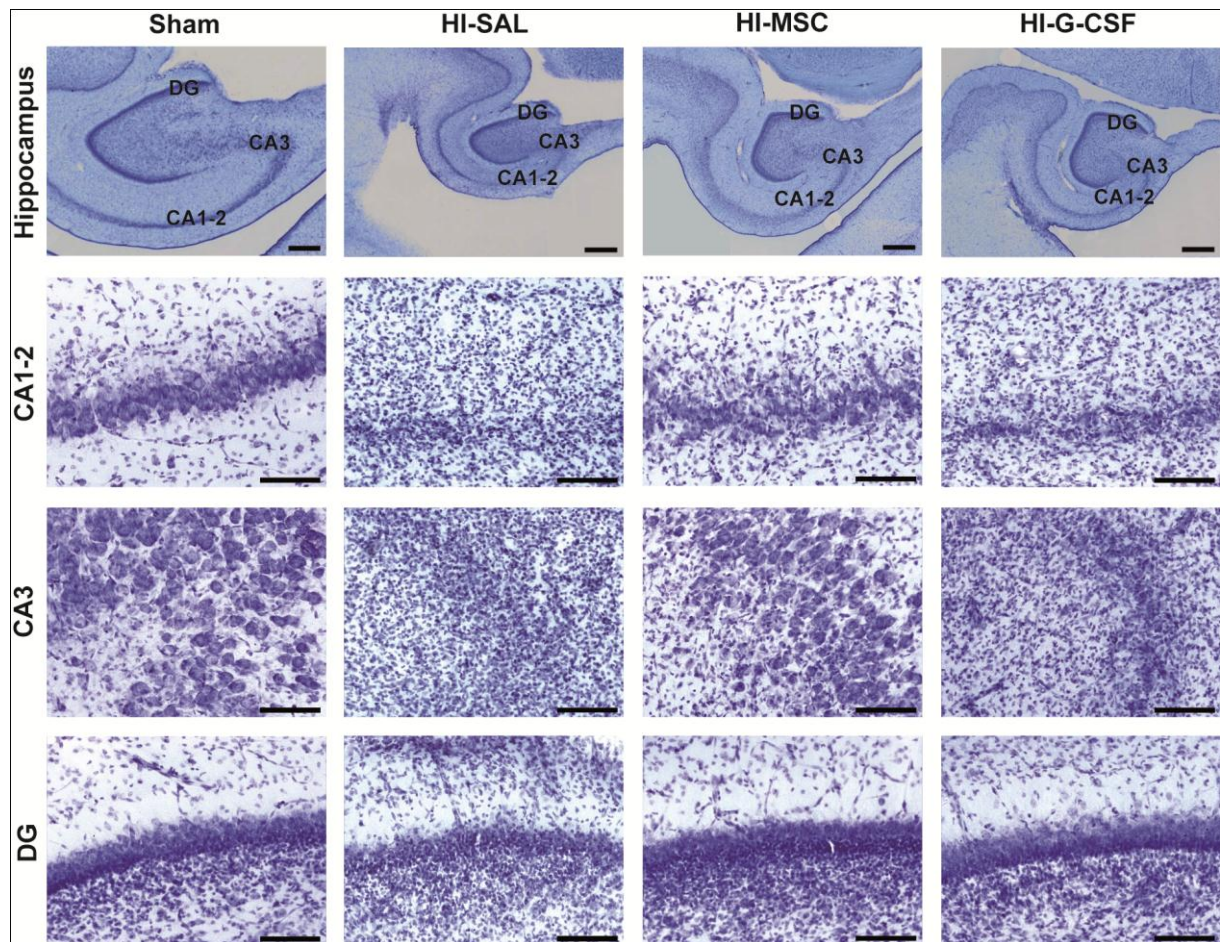


Figure 23: Nissl staining showing the SP of CA1-2 and CA3 and the SG of the DG. Note the compact SP in CA1-2 and CA3 of sham control animals and the loss of pyramidal cells in the Ammon's horn following HI. SP: stratum pyramidale, SG: stratum granulosum. Scale bar hippocampus: 500 μm . Scale bar CA1-2, CA3 and DG: 100 μm .

3.3.5 Microglial density in the hippocampus

As described in section 3.2.5, systemic HI had detrimental effects on microglial proliferation. Significant differences between sham-SAL and HI-SAL were observed in the total hippocampus as well as in all individual regions investigated. Compared to the HI-SAL group, MSC treatment in the HI group was associated with a significant reduction in the total percentage of IBA-1 expressing cells in the DG ($p=0.006$). However, when comparing sham-SAL and HI-MSC the IBA-1 stained area fraction was significantly different ($p<0.001$). In addition, when compared to occluded animals that did not receive any treatment, the MSC-occluded group showed a decreasing trend in the density of IBA-1 positive cells in CA3 (not significant). G-CSF administration after UCO slightly diminished the percentage of IBA-1 positive cells in the DG (HI-SAL vs. HI-G-CSF: $p=0.022$).

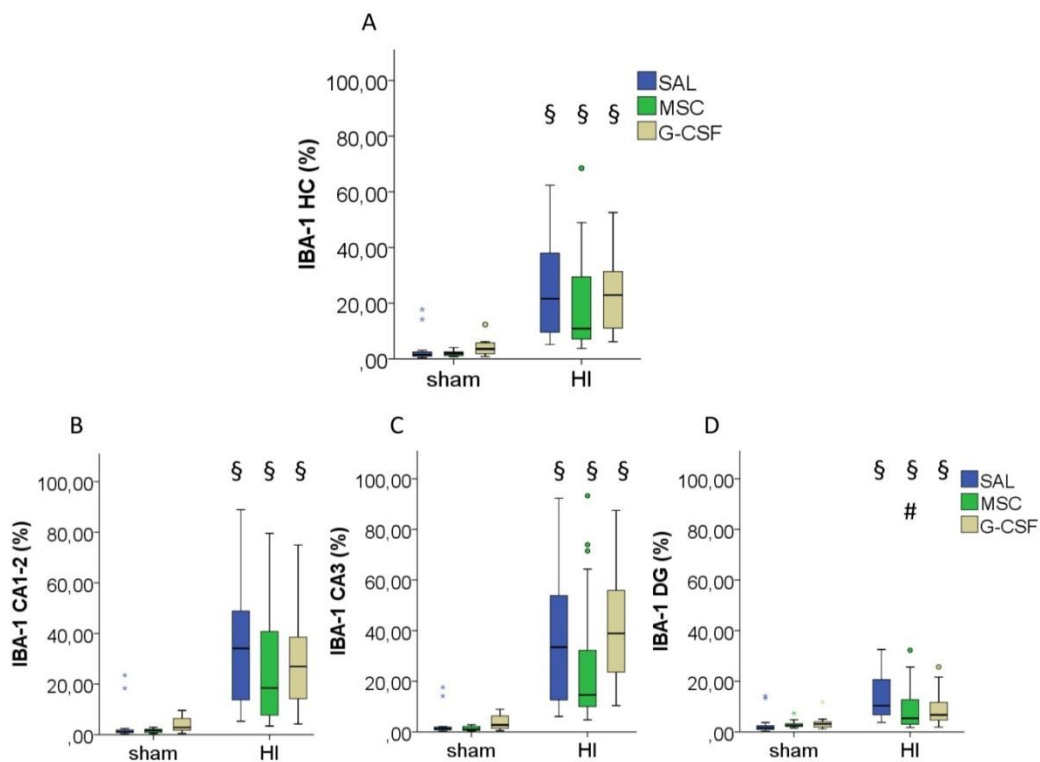


Figure 24: Area fraction (%) of IBA-1 staining in the total hippocampus (A) and CA1-2, CA3 and DG (B – D) for all experimental groups. Global HI was associated with a massive increase in microglial density in all regions of the hippocampal formation. MSC and G-CSF administration did not have a significant influence on IBA-1 density in hippocampal regions CA1-2 and CA3. In the DG, G-CSF treatment following UCO showed moderate effects on microglial density, while MSC therapy significantly reduced the % of IBA-1 staining. However, the overall effect of MSC administration after occlusion on the DG is minor. § $p<0.01$ (compared to sham-SAL), # $p<0.01$ (compared to HI-SAL).

Table 5: Comparison of means of IBA-1 staining (%) with Mann-Whitney U test and Bonferroni correction. P-values of comparisons are shown for the total hippocampus and for all hippocampal regions investigated.

	IBA-1 (%)			
	HC	CA1-2	CA3	DG
sham-SAL vs. HI-SAL	0.000*	0.000*	0.000*	0.000*
sham-SAL vs. HI-MSC	0.000*	0.000*	0.000*	0.000*
sham-SAL vs. HI-G-CSF	0.000*	0.000*	0.000*	0.000*
HI-SAL vs. HI-MSC	0.065	0.118	0.071	0.006*
HI-SAL vs. HI-G-CSF	0.895	0.423	0.396	0.022 [§]

* p<0.01 (Bonferroni correction: level of significance: 0.05/5 = 0.01)
[§] p<0.05

Microglia in the hippocampi of sham animals exhibited a quiescent state characterized by thin processes. In contrast, cells with tick cell bodies and retracted processes were observed in the HI-SAL group. This was accompanied by clear increase in cell density. Representative pictures of hippocampi in the HI-MSC and HI-G-CSF groups both showed a decrease in microglial proliferation. Compared to sham-SAL, cells with activated characteristics were present in both treatment groups. In addition, focal collections of reactive microglia were observed throughout the hippocampus. In all experimental groups, it was striking that less microglia were present in the DG (figure 25).

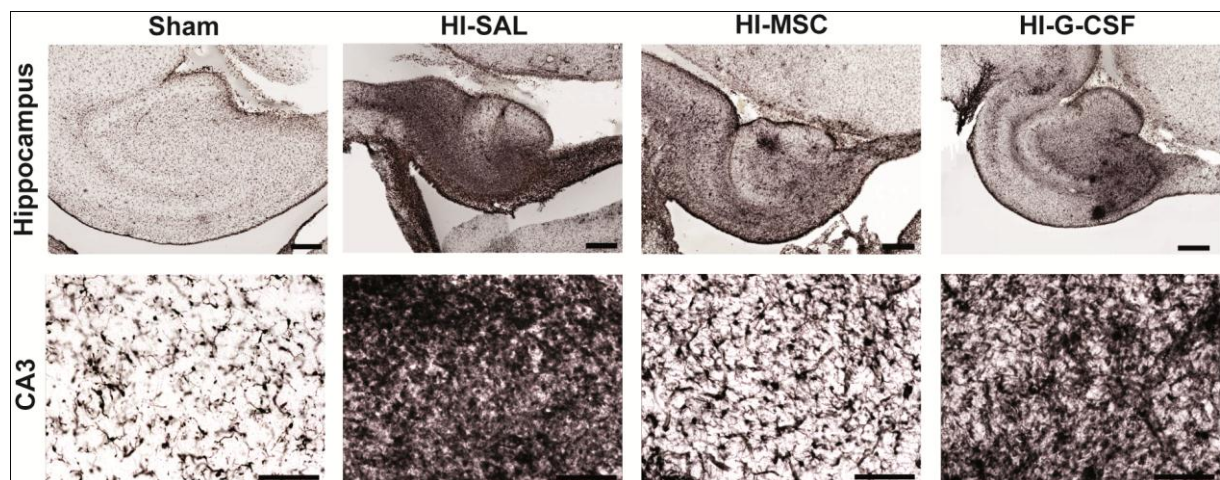


Figure 25: Representative photomicrographs showing microglial proliferation and activation. IBA-1 immunohistochemistry revealed profound microglial proliferation and activation after global HI. Cell proliferation as well as activation was somewhat decreased in the MSC and G-CSF occluded groups. Scale bar hippocampus: 500 µm. Scale bar: 100 µm.

3.3.6 Microglial density in the periventricular white matter

As is the case in the hippocampus, our results demonstrate a significant increase in microglial density in the PVWM of animals subjected to systemic HI (sham-SAL vs. HI-SAL: $p=0.008$). The percentage of IBA-1 positive cells did not significantly differ between the MSC-occlusion group and the group that did not receive any treatment after UCO ($p=0.605$). Though, a decreasing trend in microglial density was observed when comparing the sham-SAL and the HI-MSC group. This trend did not reach the level of significance ($p=0.024$), probably due to high variance. The effects of G-CSF administration on microglial density in the PVWM was not determined.

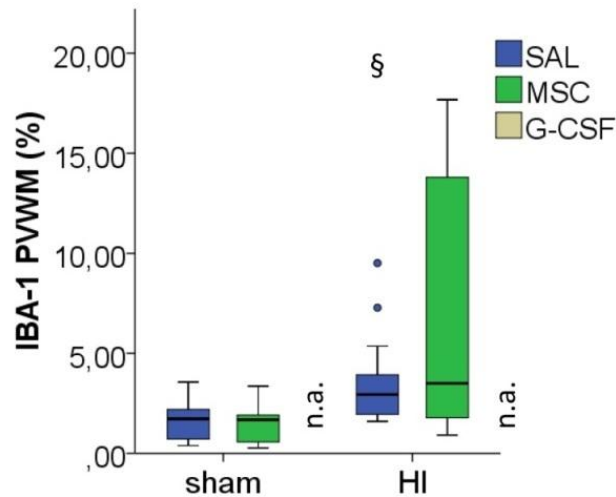


Figure 26: Area fraction of IBA-1 staining (%) in the PVWM for all experimental groups. Systemic HI was associated with a significant increase in microglial density in the PVWM. Values between HI-SAL and HI-MSC were not significantly different ($p=0.605$). The effects of G-CSF administration on microglial density in the PVWM was not determined. N.a. = not analyzed. § $p<0.01$ (compared to sham-SAL).

Table 6: Comparison of means of IBA-1 staining (%) with Mann-Whitney U test with Bonferroni correction. P-values of comparisons are shown for the PVWM.

	IBA-1 PVWM (%)
sham-SAL vs. HI-SAL	0.008*
sham-SAL vs. HI-MSC	0.024 [§]
HI-SAL vs. MSC HI-MSC	0.605
* $p<0.017$ (Bonferroni correction: level of significance: $0.05/3 = 0.017$)	
[§] $p<0.05$	

Results obtained from densitometric analysis were confirmed in pictures showing the morphological characteristic of microglial cell in three experimental groups (Sham, HI-SAL and HI-MSC). IBA-1 immunohistochemistry revealed profound microglial proliferation in the PVWM of occluded fetal sheep. Additionally, morphological changes of microglia from the resting to the activated state were detected. As illustrated by the right picture, the PVWM of the MSC-occlusion group showed a decrease in microglial density when compared to the same region in the HI-SAL group. However, compared to sham, cells appeared to be more active.

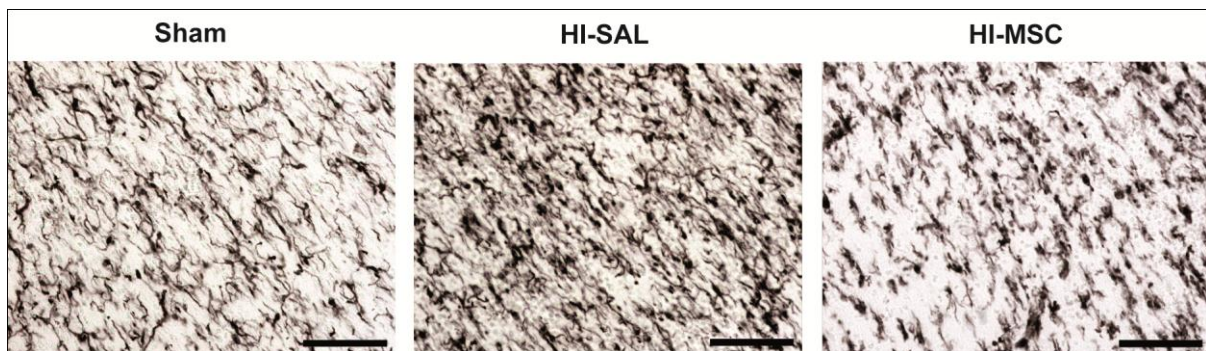


Figure 27: IBA-1 immunohistochemistry in the PVWM of sham, HI-SAL and HI-MSC experimental groups. Photomicrographs show a shift from resting microglia to an activated cellular state in HI-SAL. Compared to HI-SAL, MSC administration was associated with a decreased cell density a diminished state of activity. Scale bar = 100 μ m.

3.3.7 White matter O4 expression

Analysis of the PVWM revealed a significant loss of pre-oligodendrocytes after UCO (sham-SAL vs. HI-SAL: $p < 0.001$). Compared to the HI-SAL group, a significant increase in the number of O4 positive cells was observed in the MSC-occlusion group ($p = 0.006$). In addition, differences between sham-SAL and HI-MSC did not reach the critical level of significant ($p = 0.065$). Together, these results confirm the therapeutic effect of MSCs on pre-oligodendrocyte number.

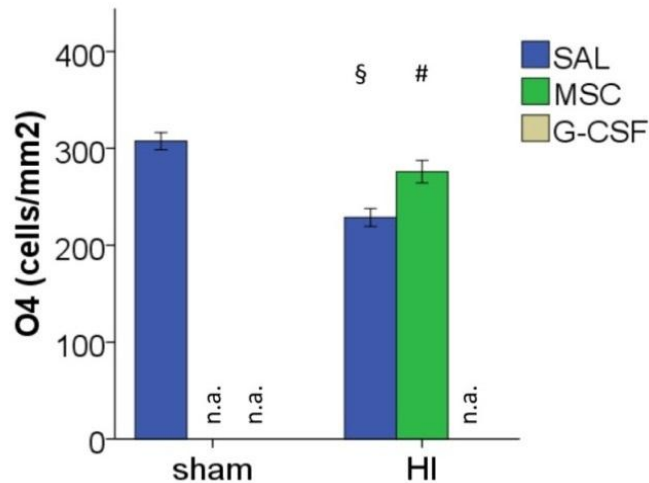


Figure 28: Number of O4 immunopositive cells (cells/mm²) in the PVWM. A significant loss of O4 positive cells was detected in the PVWM of the occluded group. Compared to HI-SAL, MSC administration after UCO is associated with a significant increase in cell number. N.a.: not analyzed. § $p < 0.01$ (compared to sham-SAL), # $p < 0.05$ (compared to HI-SAL).

Table 7: Comparison of means of O4 staining (cells/mm²) with ANOVA. P-values of comparisons are shown for the PVWM.

	O4 (cells/ mm ²)
sham-SAL vs. HI-SAL	0.000
sham-SAL vs. HI-MSC	0.065
HI-SAL vs. HI-MSC	0.006
ANOVA; sign $p < 0.05$	

Immunohistochemistry displayed O4 positive cells with a mature morphology in the PVWM of sham animals. Pre-oligodendrocyte number was visibly reduced following HI. In addition, branched processes were absent in most cells. Compared to the HI-SAL group, cell number in the MSC occlusion group increased towards control values and showed similar characteristics as cells in the sham group.

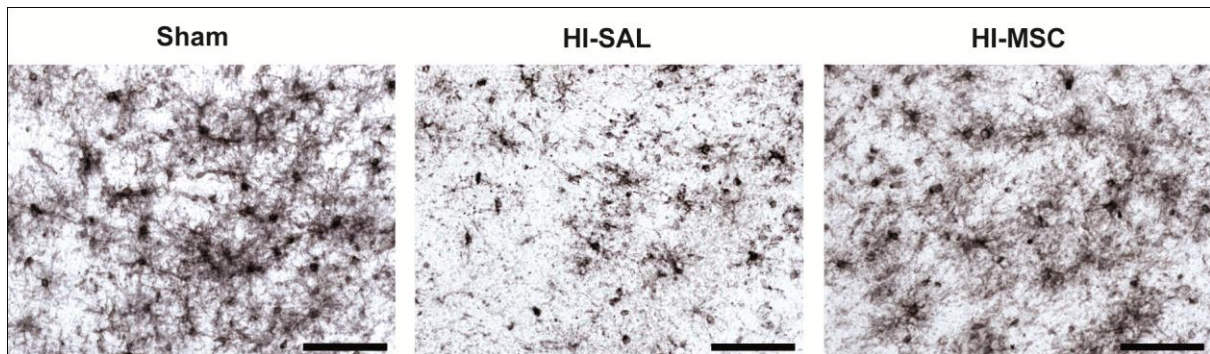


Figure 29: O4 immunohistochemistry showing pre-oligodendrocytes in the PVWM of the sham-SAL, HI-SAL and HI-MSC experimental groups. Compared to the sham-control group, global HI was associated with a reduction in pre-oligodendrocyte number. Moreover, cells displayed an immature morphology. MSC administration following UCO was accompanied by an increase in cell number. Cells showed morphological characteristics similar to those in the sham-control group. Scale bar = 100 μ m.

4. Discussion

In this translational research project the impact of global HI on synapses, neurons, microglia and pre-oligodendrocytes was determined in the fetal brain. The question that raised was: “Are exogenous administered hu-BM-MSCs and human recombinant G-CSF therapies effective in reducing brain damage, caused by a global HI insult, in a preterm sheep model?” We subsequently hypothesized that both treatments can attenuate brain injury in HI sheep fetuses, in part by reducing synapse loss, neurodegeneration, pre-oligodendrocyte loss and by diminishing the activation and proliferation of resident microglia.

The present study demonstrates that global HI in fetal sheep at midgestation results in whole brain and hippocampal atrophy. At a cellular level, we show changes in synaptic circuitries, neuronal damage and profound microglial proliferation and activation in the developing hippocampus. In addition, we present that white matter injury is associated with microglial proliferation and loss of non-myelinating pre-oligodendrocytes. Cerebral weight was preserved after MSC administration. In the hippocampus, morphology data demonstrate that MSC transplantation was associated with a reduced lesion size or clear trends towards ultrastructural repair of neurons and synaptic circuitries. In addition, MSC therapy significantly reduced the percentage of IBA-1 expressing cells in the DG and diminished microglial activation in the total hippocampus. As is the case in the hippocampus, a decreasing trend in microglial density was observed in the PVWM of the MCS-occlusion group. This was accompanied by sparing of pre-oligodendrocytes. Though less clear, G-CSF administration relatively spared the neurons and synapses in the hippocampus. Furthermore, microglial density was diminished in the DG and, when compared to HI-SAL, the cell's activity status was decreased.

The hippocampal formation is involved in learning and memory by encoding and storage of information via synaptic plasticity (61). As indicated earlier by Stracks *et al.* (2008) (62), we confirm that HI results in profound hippocampal atrophy. Our investigation provides more details on this by highlighting regional differences. Area measurements from individual hippocampal regions (CA1-2, CA3 and DG) revealed a significant decrease in the Ammon's horn of occluded animals. Judged on area data, we ascertained that the DG appeared less affected by global HI, referring to a decreased vulnerability at a GA of approximately 104 days. The fact that the immature brain has a great capacity for neurogenesis after injury (63) could be an alternative explanation for the relative sparing of the DG after HI. Both MSC or G-CSF administration did not significantly restore overall hippocampal area. When elaborating on results from individual hippocampal regions, therapies were not associated with recovering effects in the Ammon's horn. Contrary to our expectations, MSC transplantation did not have an influence on the DG area as it has been described before that treatment at three days after HI resulted in an increased cell proliferation in that region (2). Studies on MSC administration in adult stroke models have also demonstrated that MSCs transplanted at 24 hours after the insult stimulated neurogenesis at day 14 after stroke (64). It should be noted, however, that cells were transplanted intracerebrally.

Consistent with clinical imaging and post-mortem data of preterm infants (65, 66), our immunohistochemical findings demonstrate that a reversible exposure to severe hypoxia in the

preterm fetal sheep is associated with both extensive neuronal loss and changes in synaptic circuitries in the fetal hippocampus. The synaptophysin immunohistochemical staining was used for the analysis of presynaptic bouton densities. As an integral membrane protein located in presynaptic vesicles, synaptophysin is an important mediator in membrane trafficking that is frequently used as a surrogate marker to detect nerve terminals (67). Morphological data displayed a diffuse synaptophysin immunoreactivity in the Ammon's horn of fetal sheep subjected to global HI, referring to the massive neuronal loss in that region. No gross differences were observed in the DG. Furthermore, quantitative analysis of presynaptic bouton densities in the different hippocampal regions revealed that global HI was associated with a significant increase in synaptophysin expression in the CA1 SR, the CA3 SL and the DG SM. Several studies demonstrated an upsurge in pre-synaptic density in different areas of the brain immediately after an ischemic insult. For example, Fleiss *et al.* showed significant effects of global birth asphyxia on both pre- and postsynaptic expressed proteins in the neonatal rodent hippocampus (61). Likewise, Korematsu *et al.* demonstrated a transient increase in synaptophysin immunoreactivity in the rat striatum following a reversible ischemic insult (68). These results are in accordance with a study by Procianoy *et al.* (2001), wherein synaptic inactivation has been described as an initial adaptive response to HI (10). Although the exact mechanisms remain to be elucidated, an increased number of presynaptic terminals following the loss of the postsynaptic site might be an explanation. Referring to the high potential of the developing brain to adapt to injury (63), it seems plausible that cerebral injury is associated with sprouting or branching of axon terminals. These findings suggest that brain trauma, such as HI-related cerebral damage, is not only an indicator for synapse loss but can also stimulate the formation of new synaptic contacts. Alternately, when keeping compensatory mechanism in mind, an increased presynaptic activity following cerebral injury is proposed. It should be noted that the aforementioned studies refer to a transient increase in presynaptic bouton density. Several investigations examining the long-term effects of neonatal hypoxia and/or ischemia showed that synapse loss can exist a couple of weeks after the exposure. MSC and G-CSF have been shown to promote synaptogenesis in various studies. Our findings show that both MSC and G-CSF administration following UCO showed no additional effects on presynaptic bouton density in all individual hippocampal regions. These findings might indicate that the immature brains are already working at the top of their proliferative capacity and that the injury-induced proliferation in these brains could not increase beyond this level.

Results from the synaptophysin staining were supported by the Nissl staining used for the analysis of neuronal density, size and shape. Neuronal necrosis or loss in the hippocampus was confirmed by various animal models of HI injury (69, 70). Nissl staining revealed drastic neurodegenerative changes in neurons of the CA pathway, CA1-2 and CA3 pyramidal neurons, which are particularly susceptible to HI-injury (71). In contrast, the different strata of the DG were preserved and neurons of the SG showed minor ultrastructural changes. Contradictory conclusions were drawn by Towfighi *et al.* (1997), who described a relative HI-resistance of the hippocampal CA regions, whereas the DG appeared to be more vulnerable in the immature brain. Of note, cerebral lesions were studied in an immature rat model of cerebral HI. Previously, it had been suggested that structural neuronal changes may reflect a compensatory mechanism for neuronal cell loss in a particular brain region (72). It is speculated that

the relative increase in cell density observed after HI represents the proliferation of glial cells after cerebral injury. Morphological findings in the hippocampus of occluded animals that received treatment revealed that lesion extent was clearly diminished in the MSC-treated group. Results in the G-CSF-occlusion group were less outspoken but showed a trend towards ultrastructural repair. Although we did not perform quantitative analysis, these data suggest an association between MSC transplantation and neurogenesis. Based on studies on adult models of ischemic brain injury, however, it has been shown that MSC administration improved outcome by preventing neuronal loss, rather than neurogenesis (73). An alternative explanation would be that MSCs influence the brain's micro-environment, thereby allowing endogenous processes to repair the damaged tissue. As declared in several rodent models of ischemic stroke (47, 48), direct anti-apoptotic effects and the stimulation of endogenous stem cell proliferation (74) could both be responsible for the sparing of hippocampal morphology in the G-CSF occluded animals.

Concomitant with previous studies, cell loss resulting from HI was associated with intense microglial proliferation and activation in the immature brain (75). Heavily IBA-1 positive cells were present in the hippocampus and PVWM of sheep subjected to a global HI insult at a preterm age, which is a critical period for brain development. Our results demonstrate that microglial cells in the fetal hippocampus and PVWM vigorously responded to the HI insult as manifested by the increase in cell numbers and the rapid morphological alterations in which the microglial cells enlarged and their processes retracted. We suggest that this transformation was accompanied by immunophenotypic changes like the up-regulation of antigen presenting molecules (e.g. MHC II and CD80) (19). Additionally, the production of pro-inflammatory cytokines and the generation of ROS and RNS are speculated. The density of microglial cells was significantly more pronounced in the CA of the hippocampus, while less cell proliferation could be observed in the DG. Previously, a study by Ziv *et al.* (2006) revealed a close association between microglial cells, neurodegeneration and – regeneration (76). Moreover, Ekdahl *et al.* described a negative correlation between the number of surviving new hippocampal neurons and the number of activated microglia, which suggests the inhibition of neurogenesis upon microglial activation (77). Given the detrimental effects of microglial activation in post-ischemic induced early brain injury, it is important to clarify the therapeutic potential of treatments based on the inhibition of microglial activation shortly after the onset of cerebral ischemia. By reducing microglial expansion, MSC and G-CSF treatments may diminish inflammation and consequently may favour the formation of new neurons. In the fetal hippocampus, one of the most injured cerebral regions in our model, MSC and G-CSF treatments decreased the density of microglial cells in the DG, while no significant effects were observed in the Ammon's horn. Similar results were observed in the PVWM of the MSC-occlusion group. The reduced activity status, as shown by our morphological data, suggests cerebral immunomodulation by MSC therapy as it is known that MSCs can secrete several trophic factors and secretion is stimulated under post-ischemic conditions (78). To our knowledge, no comparative studies of G-CSF therapy on microglial density have been described.

Another important finding of this study is that global HI is associated with an apparent reduction in the number of pre-oligodendrocytes in the PVWM. White matter injury is one of the most frequently observed lesions in the immature brain and nearly 90% of preterm infants who develop cerebral palsy

in later life show evidence of white matter lesions (79). Using the O4 surface antigen, both late oligodendrocyte progenitors (pre-oligodendrocytes) and immature oligodendrocytes were identified in the white matter adjacent to the external angles of the lateral ventricles, a zone that is prone to injury (80, 81). Echoing *in vitro* and *in vivo* evidence (58, 82), our results demonstrate that non-myelinating oligodendrocytes are exquisitely vulnerable to HI injury. Damage to these cells results in inadequate myelin amounts and/or abnormal myelin formation with direct consequences for saltatory nerve conduction (25). In addition, photomicrographs of the PVWM of occluded animals show that the oligodendrocyte lineage maturation was markedly less advanced. Pre-oligodendrocytes with a complex multipolar morphology were detected in the PVWM of the sham-control group while cells with a simple appearance were detected in the same region of preterm sheep subjected to global HI. The theory put forward by Back *et al.* (58) suggests that the timing of appearance of pre-oligodendrocytes coincides with the high-risk period for PVWM injury. Since oligodendrocyte progenitor cells are intrinsically more sensitive to HI injury than mature myelinating cells, there is a positive relationship between the extent of preterm brain injury and the occurrence of a HI insult in time (32, 57). At a GA of 23 - 32 weeks, pre-myelinating oligodendrocytes are most abundant in the immature human brain (25). Consequently, this is a high-risk period for periventricular white matter injury. Additionally, cerebrovascular immaturity had been proposed as another potential mechanism for PVWM damage. In the immature brain, the PVWM is situated between the end zones of the arterial vascular supply and therefore might be particularly affected by cerebral hypoperfusion (83). As demonstrated by *in vitro* experiments, immature oligodendrocytes are highly susceptible to oxygen and glucose withdrawal (84). In addition, these cells are extremely vulnerable to free radical attack, excitotoxicity and microglial activation, three downstream mechanisms of an HI insult (85). Remyelination is indispensable in restoring axonal conductance and consequently for functional recovery after HI brain injury. We demonstrated that MSC administration has the ability to prevent and/or restore HI-related white matter lesions. The increase in pre-oligodendrocyte number in the HI-MSC group was in accordance with a study of van Velthoven *et al.* (2010) (2), who described an association between MSC treatment and an enhanced differentiation of proliferating cells towards oligodendrocytes.

A gross advantage of regenerative therapies is the broad therapeutic window as cell transplantation has been shown to act neuroprotective when treatment was started for up to 24 hours after the onset of ischemic brain injury (86). Based on previous investigations, we suggested that therapies could reach the injured brain with preferable homing in the ischemic cerebral areas. Unfortunately, we were not able to show this in the present investigation. Moreover, as described in a study by van Velthoven *et al.* (2010) (2), endogenous repair mechanisms start to be active within two to three days after the insult, suggesting that this is the optimal time point to start treatment. In our study, MSC therapy was given one hour following the insult, which might suggest that at that time the brain is not favoring regenerative processes. It might also be possible that the number of transplanted cells or the amount of G-CSF administered is too little in relation to lesion volume. Continuing this, it is essential to know how many cells actually reach the preterm brain and the other organs in which the cells end up when administered *i.v.* Moreover, cell differentiation and survival after transplantation are two other important issues that need to be addressed. Certainly, the promising results of cell therapy in preterm

sheep can be regarded as the first step in the developing of a therapeutic approach for future clinical use. However, in order to enable the translation of experimental research into clinical practice, many issues should be kept in mind. First of all, it is noteworthy that mechanisms of damage and regeneration are more complex in human brain diseases. Furthermore, when applying neuroprotective strategies, it is important to ascertain the time window available to start treatment. Although reduced brain damage and/or advances in sensimotor and cognitive outcome in experimental animals have been described for several neuroprotective strategies, it should be kept in mind that many agents have only been shown efficient when administered before or immediately after the insult. This is a problem, since both the onset and the timing of HI cannot be ascertained in the clinic. Additionally, issues related to cell types and the route of delivery need to be determined. In order to provide a basis for clinical use, dose-response analysis of stem cells need to be performed in animal models. Further studies on the working mechanisms of stem cells in HI injury are crucial in establishing transplantation effectiveness and safety.

5. Conclusion and synthesis

In the present study, the potential of stem cell therapy in preterm HI injury was explored. We showed that UCO for 25 minutes resulted in substantial acidemia, hypoxemia, hypercapnia, bradycardia and hypotension. EEG measurements revealed severe brain dysfunction following the HI episode (data not shown). Additional data showed a significant decrease in cerebral weight of occluded animals. Our immunohistochemical findings show selective vulnerability of the hippocampus and PVWM following systemic HI in the preterm brain. This is in accordance with clinical findings in preterm infants suffering from HI insults. Furthermore global HI was associated with severe neuronal loss in the hippocampus and marked microglial proliferation in both hippocampus and PVWM. Moreover, in the PVWM, HI resulted in significant loss of immature oligodendrocytes. Together, these results ascertain the establishment of a unique and reproducible ovine model of preterm HIE. Our findings show that the instrumented preterm sheep model is a strong translational tool to test cell-based therapies in preterm HI brain injury, since the model shares many developmental and pathophysiological features with the human situation.

Our data show that exogenous MSCs transplantation diminished brain atrophy and prevented EEG suppression (i.e. reduced brain function) after global HI (preliminary data, not shown in this thesis). Our findings indicate that MSC and G-CSF therapies were associated with mild improvements at a cellular level. Nevertheless, both cell-based therapies were accompanied by clear trends toward ultrastructural repair of neurons and synaptic circuitries in the hippocampus and a slight decrease in microglial activation and proliferation. In addition, MSC therapy following global HI was accompanied by a significant increase in pre-oligodendrocyte number in the PVWM. In conclusion, MSC and G-CSF therapy had mild neuroprotective effects on the preterm brain following HI.

The implementation of stem cell therapy in perinatal practice requires the establishment of optimal timing, dose and route of administration in experimental and pre-clinical studies. Although many issues still need to be addressed, stem cell transplantation is a promising candidate to become a future neuroprotective therapy for HI brain damage in preterm infants.

References

1. Kehrer M, Blumenstock G, Eehalt S, Goelz R, Poets C, Schoning M. Development of cerebral blood flow volume in preterm neonates during the first two weeks of life. *Pediatric research*. 2005;58(5):927-30. Epub 2005/09/27.
2. van Velthoven CT, Kavelaars A, van Bel F, Heijnen CJ. Mesenchymal stem cell treatment after neonatal hypoxic-ischemic brain injury improves behavioral outcome and induces neuronal and oligodendrocyte regeneration. *Brain, behavior, and immunity*. 2010;24(3):387-93. Epub 2009/11/04.
3. Lawn JE, Manandhar A, Haws RA, Darmstadt GL. Reducing one million child deaths from birth asphyxia--a survey of health systems gaps and priorities. *Health research policy and systems / BioMed Central*. 2007;5:4. Epub 2007/05/18.
4. Beck S, Wojdyla D, Say L, Betran AP, Merialdi M, Requejo JH, et al. The worldwide incidence of preterm birth: a systematic review of maternal mortality and morbidity. *Bulletin of the World Health Organization*. 2010;88(1):31-8. Epub 2010/04/30.
5. de Haan M, Wyatt JS, Roth S, Vargha-Khadem F, Gadian D, Mishkin M. Brain and cognitive-behavioural development after asphyxia at term birth. *Developmental science*. 2006;9(4):350-8. Epub 2006/06/13.
6. Graham EM, Ruis KA, Hartman AL, Northington FJ, Fox HE. A systematic review of the role of intrapartum hypoxia-ischemia in the causation of neonatal encephalopathy. *American journal of obstetrics and gynecology*. 2008;199(6):587-95. Epub 2008/12/17.
7. Black RE, Cousens S, Johnson HL, Lawn JE, Rudan I, Bassani DG, et al. Global, regional, and national causes of child mortality in 2008: a systematic analysis. *Lancet*. 2010;375(9730):1969-87. Epub 2010/05/15.
8. Pfister RH, Soll RF. Hypothermia for the treatment of infants with hypoxic-ischemic encephalopathy. *Journal of perinatology : official journal of the California Perinatal Association*. 2010;30 Suppl:S82-7. Epub 2010/10/12.
9. Leuthner SR, Das UG. Low Apgar scores and the definition of birth asphyxia. *Pediatric clinics of North America*. 2004;51(3):737-45. Epub 2004/05/26.
10. Procianny RS, Silveira RC. [Hypoxic-ischemic syndrome]. *Jornal de pediatria*. 2001;77 Suppl 1:S63-70. Epub 2003/12/17. *Síndrome hipoxico-isquémica*.
11. Liauw L. Hypoxic-ischaemic brain injury in young infants. *Annals of the Academy of Medicine, Singapore*. 2009;38(9):788-94. Epub 2009/10/10.
12. Wagner SR, Lanier WL. Metabolism of glucose, glycogen, and high-energy phosphates during complete cerebral ischemia. A comparison of normoglycemic, chronically hyperglycemic diabetic, and acutely hyperglycemic nondiabetic rats. *Anesthesiology*. 1994;81(6):1516-26. Epub 1994/12/01.
13. Busl KM, Greer DM. Hypoxic-ischemic brain injury: pathophysiology, neuropathology and mechanisms. *NeuroRehabilitation*. 2010;26(1):5-13. Epub 2010/02/05.
14. Quintana P, Alberi S, Hakkoum D, Muller D. Glutamate receptor changes associated with transient anoxia/hypoglycaemia in hippocampal slice cultures. *The European journal of neuroscience*. 2006;23(4):975-83. Epub 2006/03/08.
15. Ferriero DM, Holtzman DM, Black SM, Sheldon RA. Neonatal mice lacking neuronal nitric oxide synthase are less vulnerable to hypoxic-ischemic injury. *Neurobiology of disease*. 1996;3(1):64-71. Epub 1996/02/01.
16. Teshima Y, Akao M, Li RA, Chong TH, Baumgartner WA, Johnston MV, et al. Mitochondrial ATP-sensitive potassium channel activation protects cerebellar granule neurons from apoptosis induced by oxidative stress. *Stroke; a journal of cerebral circulation*. 2003;34(7):1796-802. Epub 2003/06/07.
17. Halliwell B. Oxidative stress and neurodegeneration: where are we now? *Journal of neurochemistry*. 2006;97(6):1634-58. Epub 2006/06/30.
18. Grande Covian F. [Energy metabolism of the brain in children (author's transl)]. *Anales espanoles de pediatria*. 1979;12(3):235-44. Epub 1979/03/01. *El metabolismo energético del cerebro en la infancia*.
19. Shapiro LA, Perez ZD, Foresti ML, Arisi GM, Ribak CE. Morphological and ultrastructural features of Iba1-immunolabeled microglial cells in the hippocampal dentate gyrus. *Brain research*. 2009;1266:29-36. Epub 2009/03/03.
20. Ito D, Tanaka K, Suzuki S, Dembo T, Fukuuchi Y. Enhanced expression of Iba1, ionized calcium-binding adapter molecule 1, after transient focal cerebral ischemia in rat brain. *Stroke; a journal of cerebral circulation*. 2001;32(5):1208-15. Epub 2001/09/06.
21. Brea D, Sobrino T, Ramos-Cabrera P, Castillo J. Inflammatory and neuroimmunomodulatory changes in acute cerebral ischemia. *Cerebrovasc Dis*. 2009;27 Suppl 1:48-64. Epub 2009/04/15.
22. Gelderblom M, Leyboldt F, Steinbach K, Behrens D, Choe CU, Siler DA, et al. Temporal and spatial dynamics of cerebral immune cell accumulation in stroke. *Stroke; a journal of cerebral circulation*. 2009;40(5):1849-57. Epub 2009/03/07.
23. Ferriero DM. Neonatal brain injury. *The New England journal of medicine*. 2004;351(19):1985-95. Epub 2004/11/05.
24. Yuan TM, Yu HM. Notch signaling: key role in intrauterine infection/inflammation, embryonic development, and white matter damage? *Journal of neuroscience research*. 2010;88(3):461-8. Epub 2009/09/22.
25. Fancy SP, Harrington EP, Yuen TJ, Silbereis JC, Zhao C, Baranzini SE, et al. Axin2 as regulatory and therapeutic target in newborn brain injury and remyelination. *Nature neuroscience*. 2011;14(8):1009-16. Epub 2011/06/28.
26. Strackx E, Van den Hove DL, Steinbusch HP, Steinbusch HW, Vles JS, Blanco CE, et al. Fetal asphyxia leads to the loss of striatal presynaptic boutons in adult rats. *International journal of developmental neuroscience : the official journal of the International Society for Developmental Neuroscience*. 2010;28(3):277-81. Epub 2009/06/09.
27. Horner CH, Davies HA, Stewart MG. Hippocampal synaptic density and glutamate immunoreactivity following transient cerebral ischaemia in the chick. *The European journal of neuroscience*. 1998;10(12):3913-7. Epub 1999/01/06.
28. Hickey RW, Painter MJ. Brain injury from cardiac arrest in children. *Neurologic clinics*. 2006;24(1):147-58, viii. Epub 2006/01/31.
29. Folkerth RD. Periventricular leukomalacia: overview and recent findings. *Pediatric and developmental pathology : the official journal of the Society for Pediatric Pathology and the Paediatric Pathology Society*. 2006;9(1):3-13. Epub 2006/07/01.
30. Fatemi A, Wilson MA, Johnston MV. Hypoxic-ischemic encephalopathy in the term infant. *Clinics in perinatology*. 2009;36(4):835-58, vii. Epub 2009/12/01.
31. Yata K, Matchett GA, Tsubokawa T, Tang J, Kanamaru K, Zhang JH. Granulocyte-colony stimulating factor inhibits apoptotic neuron loss after neonatal hypoxia-ischemia in rats. *Brain research*. 2007;1145:227-38. Epub 2007/03/16.
32. Roelfsema W, Bennet L, George S, Wu D, Guan J, Veerman M, et al. Window of opportunity of cerebral hypothermia for postischemic white matter injury in the near-term fetal sheep. *Journal of cerebral blood flow and metabolism : official journal of the International Society of Cerebral Blood Flow and Metabolism*. 2004;24(8):877-86. Epub 2004/09/15.

33. Thoresen M. Cooling the newborn after asphyxia - physiological and experimental background and its clinical use. *Seminars in neonatology* : SN. 2000;5(1):61-73. Epub 2000/05/10.
34. Azzopardi D, Robertson NJ, Cowan FM, Rutherford MA, Rampling M, Edwards AD. Pilot study of treatment with whole body hypothermia for neonatal encephalopathy. *Pediatrics*. 2000;106(4):684-94. Epub 2000/10/04.
35. Paula S, Greggio S, DaCosta JC. Use of stem cells in perinatal asphyxia: from bench to bedside. *Jornal de pediatria*. 2010;86(6):451-64. Epub 2010/12/09.
36. Noh MR, Kim SK, Sun W, Park SK, Choi HC, Lim JH, et al. Neuroprotective effect of topiramate on hypoxic ischemic brain injury in neonatal rats. *Experimental neurology*. 2006;201(2):470-8. Epub 2006/08/04.
37. Sfaello I, Baud O, Arzimanoglou A, Gressens P. Topiramate prevents excitotoxic damage in the newborn rodent brain. *Neurobiology of disease*. 2005;20(3):837-48. Epub 2005/07/13.
38. Manning SM, Talos DM, Zhou C, Selip DB, Park HK, Park CJ, et al. NMDA receptor blockade with memantine attenuates white matter injury in a rat model of periventricular leukomalacia. *The Journal of neuroscience : the official journal of the Society for Neuroscience*. 2008;28(26):6670-8. Epub 2008/06/27.
39. Gould E, Reeves AJ, Graziano MS, Gross CG. Neurogenesis in the neocortex of adult primates. *Science*. 1999;286(5439):548-52. Epub 1999/10/16.
40. Eriksson PS, Perfilieva E, Bjork-Eriksson T, Alborn AM, Nordborg C, Peterson DA, et al. Neurogenesis in the adult human hippocampus. *Nature medicine*. 1998;4(11):1313-7. Epub 1998/11/11.
41. Sherman LS, Munoz J, Patel SA, Dave MA, Paige I, Rameshwar P. Moving from the laboratory bench to patients' bedside: considerations for effective therapy with stem cells. *Clinical and translational science*. 2011;4(5):380-6. Epub 2011/10/28.
42. Kohyama J, Abe H, Shimazaki T, Koizumi A, Nakashima K, Gojo S, et al. Brain from bone: efficient "meta-differentiation" of marrow stroma-derived mature osteoblasts to neurons with Noggin or a demethylating agent. *Differentiation; research in biological diversity*. 2001;68(4-5):235-44. Epub 2002/01/05.
43. Jiang Y, Jahagirdar BN, Reinhard RL, Schwartz RE, Keene CD, Ortiz-Gonzalez XR, et al. Pluripotency of mesenchymal stem cells derived from adult marrow. *Nature*. 2002;418(6893):41-9. Epub 2002/06/22.
44. Demetri GD, Griffin JD. Granulocyte colony-stimulating factor and its receptor. *Blood*. 1991;78(11):2791-808. Epub 1991/12/01.
45. Sprigg N, Bath PM, Zhao L, Willmot MR, Gray LJ, Walker MF, et al. Granulocyte-colony-stimulating factor mobilizes bone marrow stem cells in patients with subacute ischemic stroke: the Stem cell Trial of recovery EnhanceMent after Stroke (STEMS) pilot randomized, controlled trial (ISRCTN 16784092). *Stroke; a journal of cerebral circulation*. 2006;37(12):2979-83. Epub 2006/11/04.
46. Kawada H, Takizawa S, Takanashi T, Morita Y, Fujita J, Fukuda K, et al. Administration of hematopoietic cytokines in the subacute phase after cerebral infarction is effective for functional recovery facilitating proliferation of intrinsic neural stem/progenitor cells and transition of bone marrow-derived neuronal cells. *Circulation*. 2006;113(5):701-10. Epub 2006/02/08.
47. Shyu WC, Lin SZ, Yang HI, Tzeng YS, Pang CY, Yen PS, et al. Functional recovery of stroke rats induced by granulocyte colony-stimulating factor-stimulated stem cells. *Circulation*. 2004;110(13):1847-54. Epub 2004/09/24.
48. Schneider A, Kruger C, Steigleder T, Weber D, Pitzer C, Laage R, et al. The hematopoietic factor G-CSF is a neuronal ligand that counteracts programmed cell death and drives neurogenesis. *The Journal of clinical investigation*. 2005;115(8):2083-98. Epub 2005/07/12.
49. Schabitz WR, Kollmar R, Schwaninger M, Juettler E, Bardutzky J, Scholzke MN, et al. Neuroprotective effect of granulocyte colony-stimulating factor after focal cerebral ischemia. *Stroke; a journal of cerebral circulation*. 2003;34(3):745-51. Epub 2003/03/08.
50. Gibson CL, Jones NC, Prior MJ, Bath PM, Murphy SP. G-CSF suppresses edema formation and reduces interleukin-1beta expression after cerebral ischemia in mice. *Journal of neuropathology and experimental neurology*. 2005;64(9):763-9. Epub 2005/09/06.
51. Konishi Y, Chui DH, Hirose H, Kunishita T, Tabira T. Trophic effect of erythropoietin and other hematopoietic factors on central cholinergic neurons in vitro and in vivo. *Brain research*. 1993;609(1-2):29-35. Epub 1993/04/23.
52. Corti S, Locatelli F, Strazzer S, Salani S, Del Bo R, Soligo D, et al. Modulated generation of neuronal cells from bone marrow by expansion and mobilization of circulating stem cells with in vivo cytokine treatment. *Experimental neurology*. 2002;177(2):443-52. Epub 2002/11/14.
53. Six I, Gasan G, Mura E, Bordet R. Beneficial effect of pharmacological mobilization of bone marrow in experimental cerebral ischemia. *European journal of pharmacology*. 2003;458(3):327-8. Epub 2002/12/31.
54. Morris CL, Siegel E, Barlogie B, Cottler-Fox M, Lin P, Fassas A, et al. Mobilization of CD34+ cells in elderly patients (>= 70 years) with multiple myeloma: influence of age, prior therapy, platelet count and mobilization regimen. *British journal of haematology*. 2003;120(3):413-23. Epub 2003/02/13.
55. Fassas A, Passweg JR, Anagnostopoulos A, Kazis A, Kozak T, Havrdova E, et al. Hematopoietic stem cell transplantation for multiple sclerosis. A retrospective multicenter study. *Journal of neurology*. 2002;249(8):1088-97. Epub 2002/08/27.
56. Carr R, Modi N, Dore C. G-CSF and GM-CSF for treating or preventing neonatal infections. *Cochrane Database Syst Rev*. 2003(3):CD003066. Epub 2003/08/15.
57. Back SA, Riddle A, Hohimer AR. Role of instrumented fetal sheep preparations in defining the pathogenesis of human periventricular white-matter injury. *Journal of child neurology*. 2006;21(7):582-9. Epub 2006/09/15.
58. Back SA, Luo NL, Borenstein NS, Levine JM, Volpe JJ, Kinney HC. Late oligodendrocyte progenitors coincide with the developmental window of vulnerability for human perinatal white matter injury. *The Journal of neuroscience : the official journal of the Society for Neuroscience*. 2001;21(4):1302-12. Epub 2001/02/13.
59. Guillery RW, Herrup K. Quantification without pontification: choosing a method for counting objects in sectioned tissues. *The Journal of comparative neurology*. 1997;386(1):2-7. Epub 1997/09/26.
60. Jinno S, Fleischer F, Eckel S, Schmidt V, Kosaka T. Spatial arrangement of microglia in the mouse hippocampus: a stereological study in comparison with astrocytes. *Glia*. 2007;55(13):1334-47. Epub 2007/07/25.
61. Fleiss B, Coleman HA, Castillo-Melendez M, Ireland Z, Walker DW, Parkington HC. Effects of birth asphyxia on neonatal hippocampal structure and function in the spiny mouse. *International journal of developmental neuroscience : the official journal of the International Society for Developmental Neuroscience*. 2011;29(7):757-66. Epub 2011/06/07.
62. Strackx E, Van den Hove DL, Steinbusch HP, Steinbusch HW, Vles JS, Blanco CE, et al. A combined behavioral and morphological study on the effects of fetal asphyxia on the nigrostriatal dopaminergic system in adult rats. *Experimental neurology*. 2008;211(2):413-22. Epub 2008/04/12.
63. Qiu L, Zhu C, Wang X, Xu F, Eriksson PS, Nilsson M, et al. Less neurogenesis and inflammation in the immature than

- in the juvenile brain after cerebral hypoxia-ischemia. *Journal of cerebral blood flow and metabolism : official journal of the International Society of Cerebral Blood Flow and Metabolism*. 2007;27(4):785-94. Epub 2006/08/24.
64. Chen J, Li Y, Wang L, Lu M, Zhang X, Chopp M. Therapeutic benefit of intracerebral transplantation of bone marrow stromal cells after cerebral ischemia in rats. *Journal of the neurological sciences*. 2001;189(1-2):49-57. Epub 2001/09/06.
 65. Paneth N, Rudelli R, Monte W, Rodriguez E, Pinto J, Kairam R, et al. White matter necrosis in very low birth weight infants: neuropathologic and ultrasonographic findings in infants surviving six days or longer. *The Journal of pediatrics*. 1990;116(6):975-84. Epub 1990/06/01.
 66. Gilles FH, Leviton A, Golden JA, Paneth N, Rudelli RD. Groups of histopathologic abnormalities in brains of very low birthweight infants. *Journal of neuropathology and experimental neurology*. 1998;57(11):1026-34. Epub 1998/11/24.
 67. Sarnat HB, Flores-Sarnat L, Trevenen CL. Synaptophysin immunoreactivity in the human hippocampus and neocortex from 6 to 41 weeks of gestation. *Journal of neuropathology and experimental neurology*. 2010;69(3):234-45. Epub 2010/02/10.
 68. Korematsu K, Goto S, Nagahiro S, Ushio Y. Changes of immunoreactivity for synaptophysin ('protein p38') following a transient cerebral ischemia in the rat striatum. *Brain research*. 1993;616(1-2):320-4. Epub 1993/07/09.
 69. Northington FJ, Ferriero DM, Graham EM, Traystman RJ, Martin LJ. Early Neurodegeneration after Hypoxia-Ischemia in Neonatal Rat Is Necrosis while Delayed Neuronal Death Is Apoptosis. *Neurobiology of disease*. 2001;8(2):207-19. Epub 2001/04/13.
 70. Martin LJ. Neuronal cell death in nervous system development, disease, and injury (Review). *International journal of molecular medicine*. 2001;7(5):455-78. Epub 2001/04/11.
 71. Levin S, Godukhin O. Developmental changes in hyperexcitability of CA1 pyramidal neurons induced by repeated brief episodes of hypoxia in the rat hippocampal slices. *Neuroscience letters*. 2005;377(1):20-4. Epub 2005/02/22.
 72. Pal R, Oien DB, Ersen FY, Moskovitz J. Elevated levels of brain-pathologies associated with neurodegenerative diseases in the methionine sulfoxide reductase A knockout mouse. *Experimental brain research Experimentelle Hirnforschung Experimentation cerebrale*. 2007;180(4):765-74. Epub 2007/03/03.
 73. van Velthoven CT, Kavelaars A, van Bel F, Heijnen CJ. Regeneration of the ischemic brain by engineered stem cells: fuelling endogenous repair processes. *Brain research reviews*. 2009;61(1):1-13. Epub 2009/04/08.
 74. Gibson CL, Bath PM, Murphy SP. G-CSF reduces infarct volume and improves functional outcome after transient focal cerebral ischemia in mice. *Journal of cerebral blood flow and metabolism : official journal of the International Society of Cerebral Blood Flow and Metabolism*. 2005;25(4):431-9. Epub 2005/01/22.
 75. Gehrmann J, Bonnekoh P, Miyazawa T, Oschlies U, Dux E, Hossmann KA, et al. The microglial reaction in the rat hippocampus following global ischemia: immuno-electron microscopy. *Acta neuropathologica*. 1992;84(6):588-95. Epub 1992/01/01.
 76. Ziv Y, Ron N, Butovsky O, Landa G, Sudai E, Greenberg N, et al. Immune cells contribute to the maintenance of neurogenesis and spatial learning abilities in adulthood. *Nature neuroscience*. 2006;9(2):268-75. Epub 2006/01/18.
 77. Ekdahl CT, Claassen JH, Bonde S, Kokaia Z, Lindvall O. Inflammation is detrimental for neurogenesis in adult brain. *Proceedings of the National Academy of Sciences of the United States of America*. 2003;100(23):13632-7. Epub 2003/10/29.
 78. Qu R, Li Y, Gao Q, Shen L, Zhang J, Liu Z, et al. Neurotrophic and growth factor gene expression profiling of mouse bone marrow stromal cells induced by ischemic brain extracts. *Neuropathology : official journal of the Japanese Society of Neuropathology*. 2007;27(4):355-63. Epub 2007/09/29.
 79. Volpe JJ. Brain injury in the premature infant: overview of clinical aspects, neuropathology, and pathogenesis. *Seminars in pediatric neurology*. 1998;5(3):135-51. Epub 1998/10/20.
 80. Back SA, Han BH, Luo NL, Chricton CA, Xanthoudakis S, Tam J, et al. Selective vulnerability of late oligodendrocyte progenitors to hypoxia-ischemia. *The Journal of neuroscience : the official journal of the Society for Neuroscience*. 2002;22(2):455-63. Epub 2002/01/11.
 81. Mallard C, Welin AK, Peebles D, Hagberg H, Kjellmer I. White matter injury following systemic endotoxemia or asphyxia in the fetal sheep. *Neurochemical research*. 2003;28(2):215-23. Epub 2003/03/01.
 82. Bennet L, Roelfsema V, George S, Dean JM, Emerald BS, Gunn AJ. The effect of cerebral hypothermia on white and grey matter injury induced by severe hypoxia in preterm fetal sheep. *The Journal of physiology*. 2007;578(Pt 2):491-506. Epub 2006/11/11.
 83. De Reuck JL. Cerebral angioarchitecture and perinatal brain lesions in premature and full-term infants. *Acta neurologica Scandinavica*. 1984;70(6):391-5. Epub 1984/12/01.
 84. Fern R, Moller T. Rapid ischemic cell death in immature oligodendrocytes: a fatal glutamate release feedback loop. *The Journal of neuroscience : the official journal of the Society for Neuroscience*. 2000;20(1):34-42. Epub 2000/01/11.
 85. Volpe JJ, Kinney HC, Jensen FE, Rosenberg PA. The developing oligodendrocyte: key cellular target in brain injury in the premature infant. *International journal of developmental neuroscience : the official journal of the International Society for Developmental Neuroscience*. 2011;29(4):423-40. Epub 2011/03/09.
 86. Okazaki T, Magaki T, Takeda M, Kajiwara Y, Hanaya R, Sugiyama K, et al. Intravenous administration of bone marrow stromal cells increases survivin and Bcl-2 protein expression and improves sensorimotor function following ischemia in rats. *Neuroscience letters*. 2008;430(2):109-14. Epub 2007/12/07.

Acknowledgements

I am very grateful that I had the opportunity to perform an internship that combined two of my major interests, namely neuroscience and the clinical applications of stem cells. The field of neuroscience already gained my attention a few years ago whereas stem cells came into view during my first master year. The 6 months in which I performed my internship have been an enriching experience and will definitely help me to start a career in scientific research.

First and foremost I offer my sincerest gratitude to my promoter, Prof. Dr. Boris Kramer, whose expertise and understanding added considerably value to my graduate experience. I attribute the level of my Master's degree to his encouragement and effort.

Secondly, I would like to thank my co-promoter, Reint Jellema, for the help with my thesis and for allowing me the room to work in my own way. His guidance and criticism have taught me a lot during my internship and will definitely help me in the future.

Furthermore, I am very grateful to Hellen Steinbush, whose daily guidance was of great value to me. Moreover, all members of the pediatrics group have shown me the importance of working together as a team. Since science is not just black and white, it is important to share opinions and to help and support each other. My special thanks go out to Elke Kuypers and Dennis Kruk who helped me with laboratory handlings and data analysis. I recognize that this research would not have been possible without them.

Finally, I thank my parents and a cheerful group of fellow students that supported me throughout my studies.

Supplement

Supplement A

Spleen weight

Analysis of the spleen shows atrophy after global HI, suggesting a role for the peripheral immune system in HI-related cerebral injury.

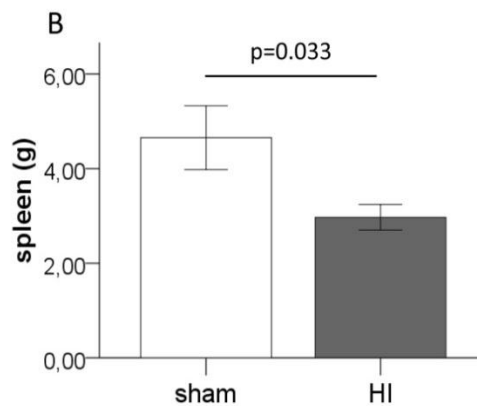


Figure 30: Global HI results in splenic atrophy. P=0.033.

Compared to other sham treated animals, splenic mass showed a profound increase in the G-CSF treated control-group. The significant reduction of splenic mass in the HI-SAL group indicates a potential role for the peripheral immune system in the pathophysiology of HI brain injury. Compared to the other treatment groups, splenic mass remained higher when occlusion was accompanied by MSC or G-CSF therapy.

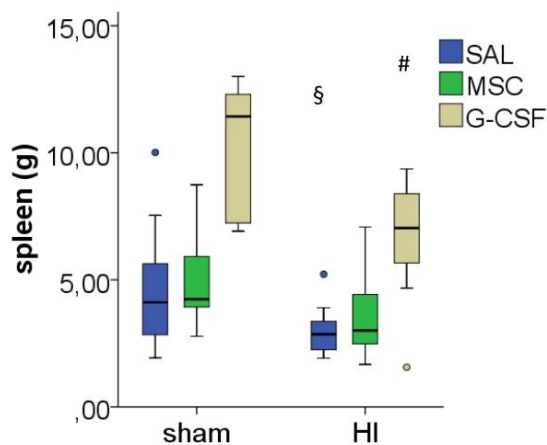


Figure 31: Spleen weight (g) for all experimental groups. Spleen weight significantly reduced following occlusion. G-CSF treatment following global HI was accompanied with a significant increase in spleen weight.

Table 8: Results of comparison of means of area with Mann-Whitney U test and Bonferroni correction. P-values of comparisons are shown for spleen weight.

	spleen (g)
sham-SAL vs. HI-SAL	0.033 [§]
sham-SAL vs. HI-MSC	0.310
sham-SAL vs. HI-G-CSF	0.128
HI-SAL vs. HI-MSC	0.583
HI-SAL vs. HI-G-CSF	0.014 [§]
* p<0.01 (Bonferroni correction: level of significance: 0.05/5 = 0.01)	
§ p<0.05	

Supplement B

Presynaptic bouton density

The effects of global HI on presynaptic bouton densities in the SR of CA1-2, the SL of CA3 and the SM of the DG are shown in figure 32 (A - F). Figure 32 A to C depicts the results of presynaptic bouton densities without correcting for synapse clustering in CA1-2, CA3 and DG respectively. With exception of CA1-2 ($p=0.001$), no overall differences were observed between both groups. Taking synapse clustering into account, analysis demonstrated no overall effect of group on bouton density. With exception of CA1-2 ($p=0.002$), all hippocampal regions in the HI group showed values that did not significantly differ from control animals (CA3; $p=0.931$, DG; $p=0.287$).

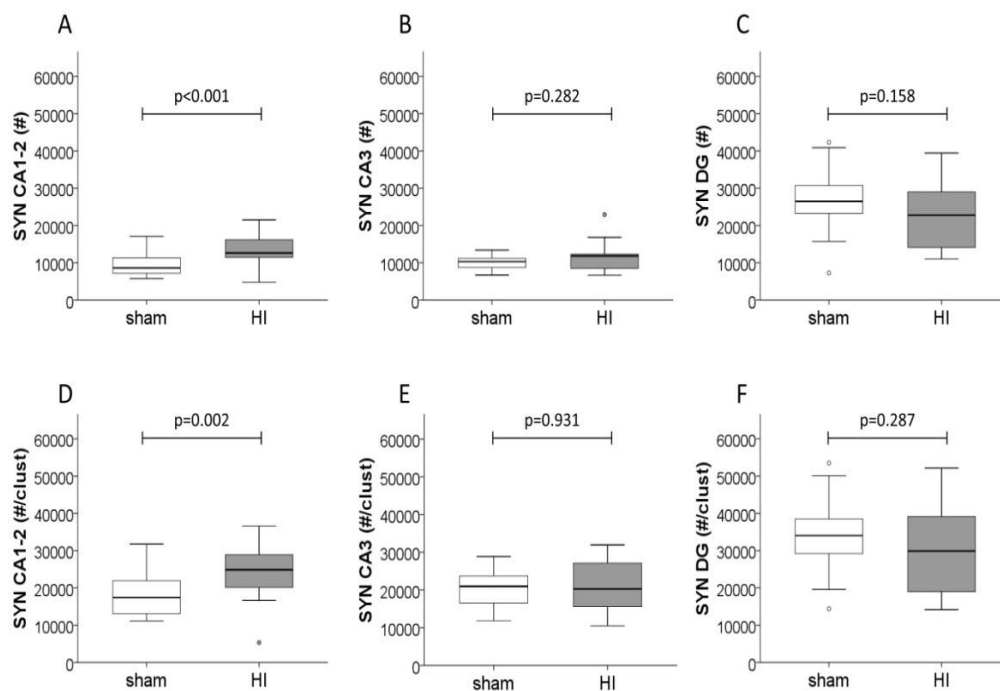


Figure 32: Synapse density ($\#/mm^2$) within CA1-2, CA3 and DG region of the hippocampus (A-C). Synapse density ($\#/mm^2$) corrected for clustering (D-F).

The effects of global HI on presynaptic bouton densities in the SR of CA1-2, the SL of CA3 and the SM of the DG are shown in figure 33 (A - F). Figure 33 A to C depicts the results of presynaptic bouton densities corrected for hippocampal area in CA1-2, CA3 and DG respectively. Significant effects between both groups were observed in all hippocampal regions. Correcting for hippocampal area and synapse clustering did not have an influence on data significance.

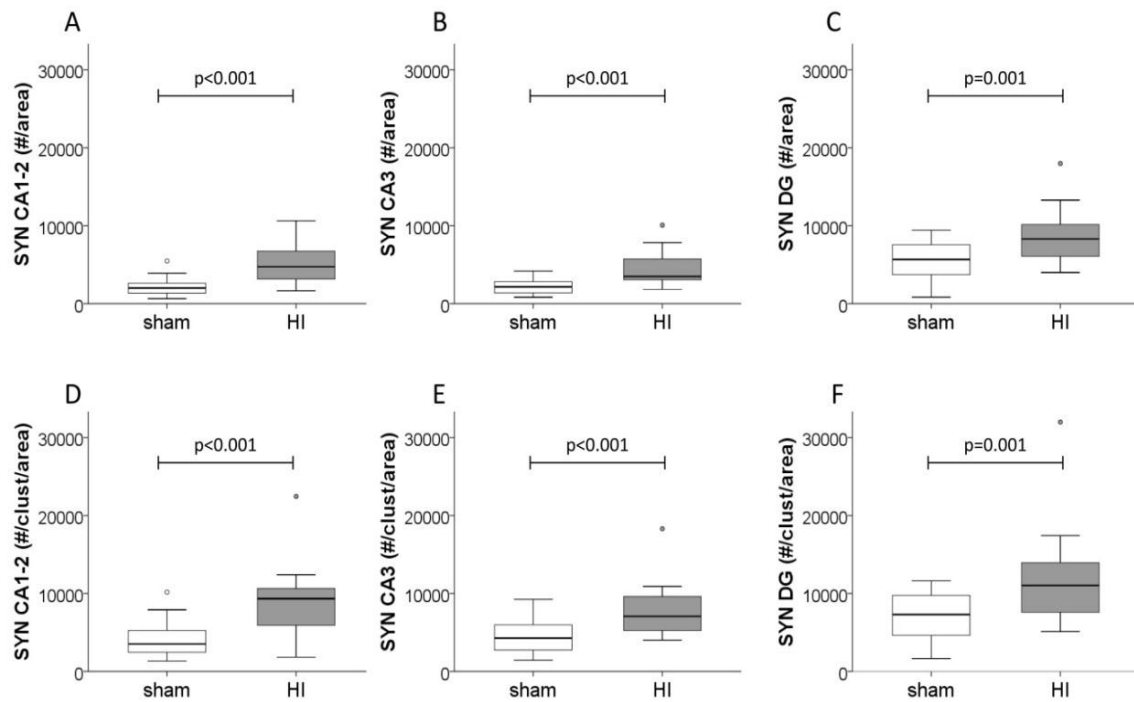


Figure 33: Synapse density ($\#/mm^2$) within CA1-2, CA3 and DG region of the hippocampus corrected for the area of the hippocampus (A-C). Synapse density ($\#/mm^2$) corrected for clustering and area of the hippocampus (D-F).

With exception of the DG, figure 34 shows no significant differences of synapse clustering between the different experimental groups.

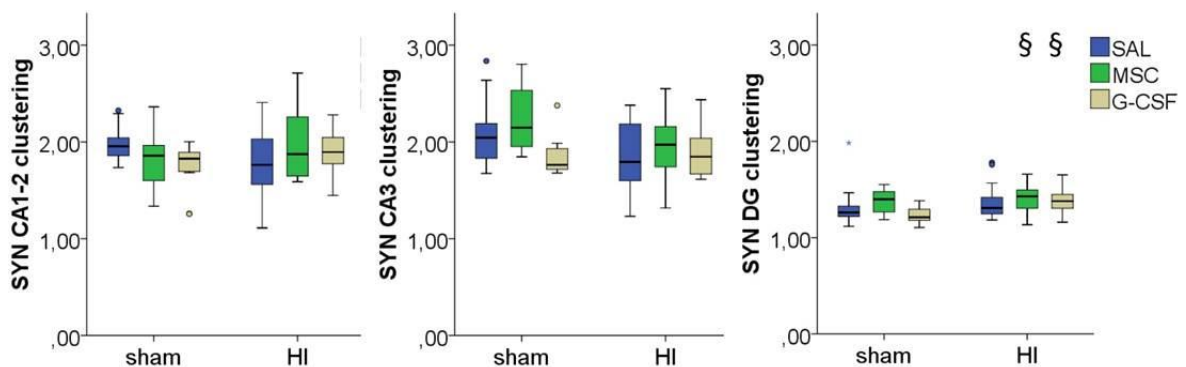


Figure 34: Synaptophysin density corrected for clustering/ synaptophysin density.

Auteursrechtelijke overeenkomst

Ik/wij verlenen het wereldwijde auteursrecht voor de ingediende eindverhandeling:

Cell therapy in neonatal hypoxic ischemic encephalopathy

Richting: **master in de biomedische wetenschappen-klinische moleculaire wetenschappen**

Jaar: **2012**

in alle mogelijke mediaformaten, - bestaande en in de toekomst te ontwikkelen - , aan de Universiteit Hasselt.

Niet tegenstaand deze toekenning van het auteursrecht aan de Universiteit Hasselt behoud ik als auteur het recht om de eindverhandeling, - in zijn geheel of gedeeltelijk -, vrij te reproduceren, (her)publiceren of distribueren zonder de toelating te moeten verkrijgen van de Universiteit Hasselt.

Ik bevestig dat de eindverhandeling mijn origineel werk is, en dat ik het recht heb om de rechten te verlenen die in deze overeenkomst worden beschreven. Ik verklaar tevens dat de eindverhandeling, naar mijn weten, het auteursrecht van anderen niet overtreedt.

Ik verklaar tevens dat ik voor het materiaal in de eindverhandeling dat beschermd wordt door het auteursrecht, de nodige toelatingen heb verkregen zodat ik deze ook aan de Universiteit Hasselt kan overdragen en dat dit duidelijk in de tekst en inhoud van de eindverhandeling werd genotificeerd.

Universiteit Hasselt zal mij als auteur(s) van de eindverhandeling identificeren en zal geen wijzigingen aanbrengen aan de eindverhandeling, uitgezonderd deze toegelaten door deze overeenkomst.

Voor akkoord,

De Munter, Stephanie

Datum: **12/06/2012**